Alma Mater Studiorum – Università di Bologna

DOTTORATO DI RICERCA in BIOCHIMICA

XXI Ciclo

Settore scientifico disciplinare di afferenza: BIO 12

Expression and cellular localization of Copper transporter 2 (Ctr2) in *Mus musculus*

Presentata da:

Stefano Cottignoli

Coordinatore Dottorato:

Chiar.mo Prof. Giorgio Lenaz

Relatore:

Chiar.mo Prof. Emilio Carpenè

Esame finale anno 2009

1 Introduction

1.1 Overview on molecular biology of copper homeostasis

Copper (Cu) is a redox-active metal ion than can exist in two forms, Cu(I) and Cu (II). Copper is an essential trace metal in biology employed as a catalytic and structural cofactor in many metalloproteins involved in different biological processes such as energy generation, iron transport, signal transduction, blood coagulation and more (Kim et al., 2008). It is likely that thus far only a part of the copper binding proteins have been discovered and characterized, since by bioinformatics analysis Andreini et al. (2008) estimated that around 1% of the total bacterial and eukaryotic proteomes is composed by Cu binding proteins.
It is well known that given its redox properties copper can also lead to toxicity especially in case of over accumulation (Gaetke and Chow CK, 2003). Not surprisingly all organisms have evolved a complex and efficient machinery to uptake, distribute and excrete this metal, leaving no free copper ions in the cell (Rea et al., 1999).
The inability to control Cu balance is associated with genetic diseases of overload and deficiency and has recently been tied to neurodegenerative disorders and fungal virulence (Kim et al., 2008).
In general proteins involved in copper homeostasis can be divided in two main and broad categories: copper chaperones and membrane transporters.
Copper delivery and distribution within the cell is mediated by a family of proteins termed metallochaperones that function to provide copper directly to target pathways while protecting this metal from intracellular scavenging (O'Halloran and Culotta, 2000).
Copper membrane transporters are membrane integral proteins that mediate the copper transfer across biological membranes (Prohaska, 2008).
In the current model of copper homeostasis in higher organisms Ctr1 (Copper transporter 1 represents the main route of copper entry into the cells. Despite Ctr1 is the only high affinity copper transporter identified so far, two lines of evidence suggest the existence of Ctr1 alternative copper uptake pathway: embryonic fibroblast Ctr1 null exhibits a residual (around 25% compared to wild type fibroblast) copper uptake activity (Lee et al., 2002b) and mice heterozygous for Ctr1 exhibit copper accumulation defects only in specific tissues (Kuo et al., 2001; Lee et al., 2001).
Recently a role for Ctr2 in mobilizing intracellular copper stores or mediating copper uptake from the plasma membrane was proposed (van den Berghe et al., 2007; Bertinato et al., 2008).
Once copper enters in the cytoplasm it can be directed to three main routes (Fig. 1).
The first involves copper delivery to the mitochondria. The matrix of this compartment has been shown to contain a Cu storage pool that can be used either for the metallation of the two more abundant copper binding mitochondrial proteins, CcO (cytochrome C oxidase) and SOD1 (Superoxidase dismutase) or for export into the cytosol (Cobin et al., 2004, Cobin et al., 2006).
A central actor in this pathway is the copper chaperone Cox17 (Cytochrome c oxidase 17), located in the mitochondrial membrane space, which is required for Cytochrome Oxidase assembly and has been proposed to deliver copper to Cu_B of Cox1 (Cytochrome c oxidase complex 1) via Cox11 (Cytochrome c oxidase 11), and to Cu_A of Cox2 (Cytochrome oxidase complex 2) via Sco1 (Cynthesis of cytochrome c oxidase 1) ((Horng et al., 2004).
In mammals Cox17 is an essential protein, indeed Cox17 null mice are embryonic lethal (Takahashi et al., 2002). Mitochondrial copper levels are unchanged in yeast cells depleted for Cox17, therefore other biomolecules delivering copper to these organelles must exist. The authors proposed that the same ligand binding copper in the matrix act as a copper shuttle in

and out the mitochondria (Cobin et al., 2004; Cobin et al., 2006). The biochemical nature of such ligand is currently under investigation.
The second route is the delivery of copper to the Golgi compartment, where the metallation of holo newly synthesized metalloproteins takes place, turning them into the active and final apo forms.
Two main proteins involved in copper delivery to the Golgi lumen have been characterized: Atox1 (Antioxidant protein 1) is cytosolic copper chaperone that delivers copper by direct interaction to ATP7a and ATP7b, which in turn mediate the transfer of the metal across the Golgi membranes (Hamza et al., 1999). The copper mediated interaction between Atox1 and N-terminal domain ATP7 (ATPase) is probably the most studied and best structurally characterized example of delivery of copper from one protein to another (Wernimont et al., 2000; Banci et al., 2006; Banci et al., 2009).
Atox1, as Cox 17, is essential for embryonic development (Hazma et al., 2003) and very recent publications suggest an alternative role for Atox1 in copper homeostasis as copper responsive transcription factor involved in cell proliferation (Itoh at al., 2008; Itoh et al., 2009).
ATP7a and b are copper specific P(1B)-type ATPases (Argüello et al., 2007) that have been extensively studied during the last two decades. These transporters are not only involved in copper delivery to the secretory pathway but play an essential role in excreting copper excess out of the cells and tissue (Lutsenko et al., 2008). Indeed mutations of ATP7a lead to Menkes disease, a X-linked lethal disorder characterized by intestinal Cu overaccumulation and concomitant copper deficiency in peripheral tissues, while mutations of ATP7A are responsible for Wilson's disease, an autosomal recessive disease characterized by hepatotoxicity and neurotoxicity due to copper overload in these tissues (Madsen and Gitlin, 2007).
The third pathway is the delivery of copper to cytosolic proteins, the most abundant of which is SOD1.
A copper chaperon renamed CCS (copper chaperon for SOD1) mediates post-translational SOD1 activation by copper loading and oxygen dependent formation of an intra-molecular disulfide bond in the enzyme (Brown et al., 2004; Furukawa et al., 2004). These observations are consistent with a role for CCS in activating SOD in response to oxidative stress.
Amyotrophic lateral sclerosis (ALS) is a neurodegenerative disease caused by distinct mutations in the SOD1 gene, all causing neurotoxicity. Despite many mutations causing the disease have been mapped some of them do not seem to affect the biochemical and enzymatic activities of SOD1 (Potter and Valentine, 2003). Recently in mouse model for ALS the overexpression of CCS was associated with mitochondrial pathology acceleration of the disease course (Son et al., 2007), suggesting that this protein could have a role in this disease.
Both CCS and SOD1 are found not only in the cytosol but also in the mitochondrial intermembrane space (IMS), from where they probably protect the cells by the superoxide ions during the mitochondrial electron transport reactions (Sturtz et al., 2001).
CCS differently from Cox17 and Atox1 is not an essential protein interestingly CCS null mice are viable and retain partial SOD1 activity, suggesting the existence of CCS copper loading and SOD1 independent activation pathway (Wong et al., 2000). Several lines of evidence support confirm this hypothesis, in particular the genome of the worm *Caenorhabditis elegans* does not code for CCS but this organism synthesizes fully active forms of the enzyme (Jensen and Culotta, 2005). Metallation of extracellular SOD (eSOD or SOD3) a form secreted in the extracellular environment has been shown to be dependent on the Atox1/ATP7a pathway (Qin et al., 2006).
This observation and the lack of observed CCS localization to the TGN suggest the possibility that the CCS independent SOD1 metallation/activation may take place in the secretory pathway.

CCS expression levels are inversely proportional to copper availability; indeed copper excess leads to a proteasome dependent degradation of the CCS (Bertinato J, L'Abbé MR). Despite this regulation has been shown to be uncoupled from the ability to load copper onto the apoSOD1 (Caruano-Yzermans et al., 2006) the role of this regulation in copper homeostasis in not well understood.
MT (Metallothionein) is a low molecular weight (6-7kDa) non-enzymatic protein ubiquitous in the animal kingdom that performs a wide array of biological functions (Carpene' et al., 2007). Its central role in copper is highlighted by studies that suggest the importance of this protein as copper sink in case of copper hyper accumulation (Suzuki, 1995) as well as its protective role, not yet elucidated, during copper starvation (Ogra et al., 2006). The partners that interact and exchange copper ions with metallothioneins have not been yet identified.
Many questions regarding molecular machinery regulating copper homeostasis still need to be answered, but probably the "one million dollar" in this research field is how the cells can sense even minimal variations in copper concentration. Despite many researchers have hypothesized the existence of a "copper sensor" such protein has not been identified yet.

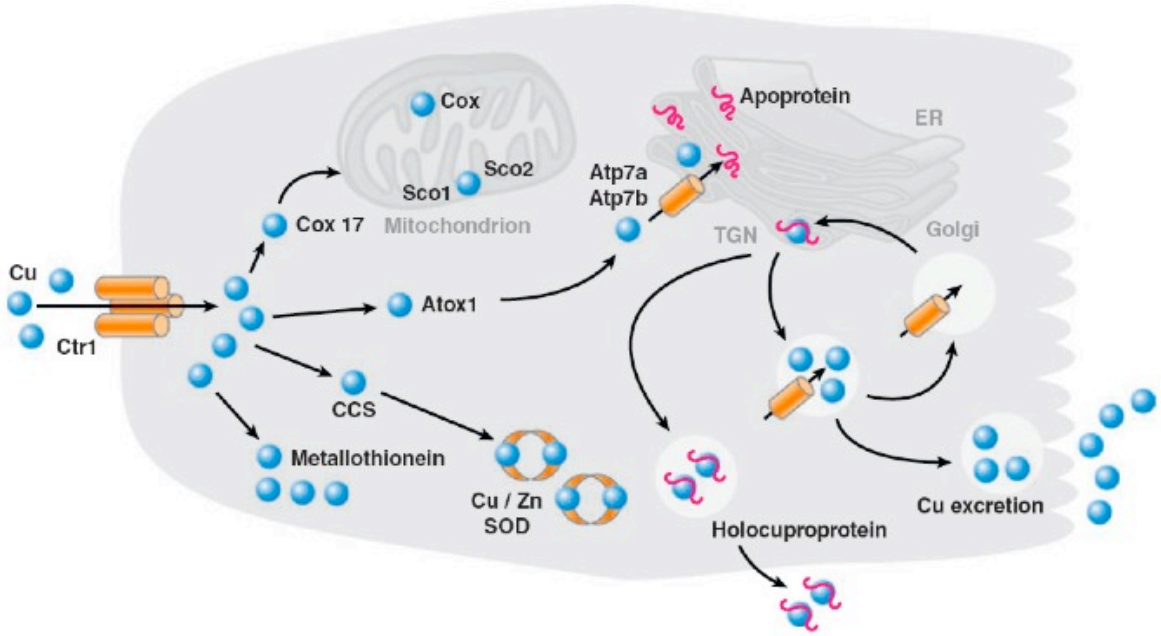

Figure 1. Schematic representation of copper homeostasis in animal cells.

1.2 Copper transporter (Ctr) proteins

In the last decades studies developed by many groups have succeeded in the identification of proteins belonging to the Ctr family throughout the whole eukaryotic kingdom.
Ctr proteins are the only high affinity copper transporter identified so far in higher organisms, but their mechanism of action is still unknown.
The first Ctr protein was described and characterized in yeast during the early 90s (Dancis et al., 1994) and since then this organism has been a model to identify through complementation

studies Ctr hortologues in plants (Kampfenkel at al., 1995) in human (Zhou and Gitschier, 1997), mouse (Lee et al., 2000) and lizard (Riggio et al., 2002).
Recently by informatic approach (Dumay et al., 2006) it was observed that despite length of the Ctr protein can greatly vary among different species, all Ctr sequences share two characteristic features (Fig. 2a):

1) the presence of three putative transmembrane domains (TMD) the first distant from the second two, which are close to each other in the linear sequences of these proteins.
2) a very high conserved aminoacid sequence located between TMD2 and TMD3 (Dumay et al., 2006):

   (YF) $(Hy)_2$ **M** $(Hy)_3$ **M** (TSY) (YF) N X_2 $(Hy)_8$ **G** $(Hy)_3$ G X $(Hy)_3$

   where Hy are hydrophobic residues and X are any residues.

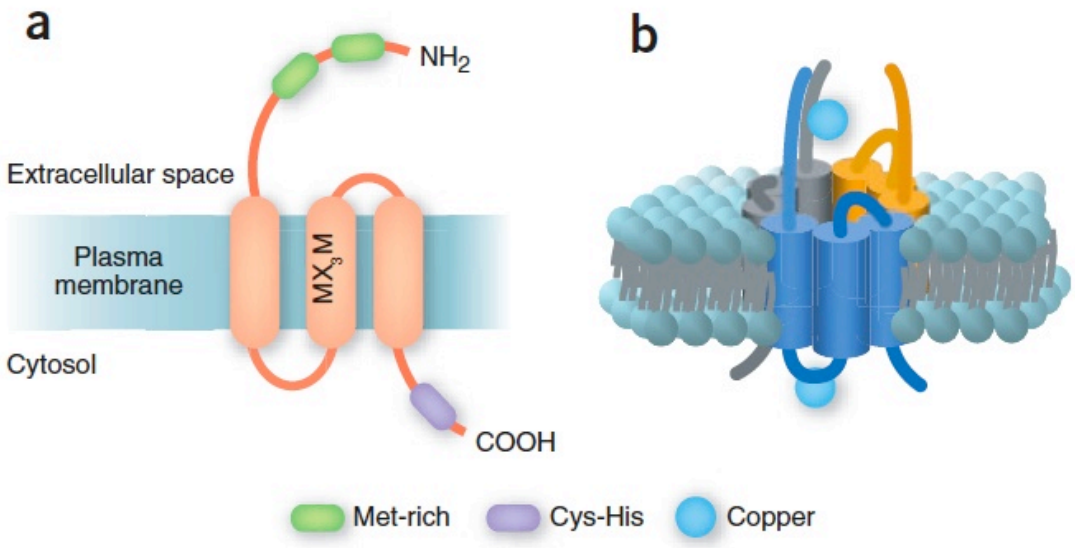

Figure 2. a) Schematic representation of topology of the Ctr1 monomer highlighting the three TMDs and Met-rich and Cys-His putative copper binding sites. b) Model for Ctr1 trimer embedded in the plasma membrane.

Furthermore while genomes of lower eukaryotes contain usually three or more members belonging to this family, vertebrates code for no more than two Ctr proteins (Dumay et al., 2006).
Ctr mediated high affinity copper transport was demonstrated mainly by studies involving incorporation of Cu^{64} in different cell lines (Lee et al., 2002a; Eisses and Kaplan, 2005b).
In the last decade human Ctr1 (hCtr1) has become the model to elucidate structure, regulation and physiological role of these proteins in copper homeostasis of these proteins in vertebrates.

1.2.1 Human Copper transporter 1 (hCtr1) structure

Only very recently the structure of the hCtr1 has been resolved by electron crystallography, confirming what previously hypothesized, that three hCtr1 molecules pack tail-to-tail forming a pore at the center of the trimer (Lee et al., 2002a; Eisses and Kaplan, 2002).
Each monomer spans the membrane layer three times forming a cone shaped pore: at the extracellular end, the pore is narrow and only the TMD2 from each monomer contributes to its lining, while following rearrangement of helix packing at the intracellular end it widens with all three TMD distributing evenly around it define its shape (De Feo et al., 2009) as shown in Fig. 3.
The TMD3 helix, almost perpendicular to the membrane plane, is connected to TMD2 by a short loop, only three aminoacids, on the extracellular sides, and can approach the helix in the TMD1 very tightly, supporting the idea that is important for helix packing, as previously suggested by mutation analysis of the very well conserved GXXXG motif in this domain (Aller et al., 2004).

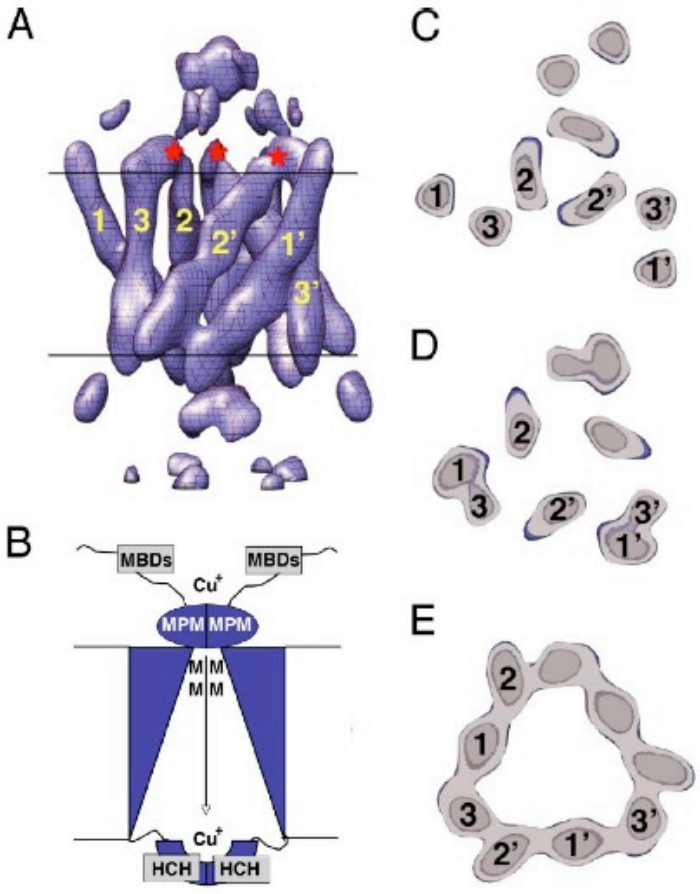

Figure 3. A) Tridimensional side view of hCtr1 trimer. Red asterisk indicates the short extracellular loop between TMD2 and TMD3. The main copper binding sites are reported. B) Schematic view of the conical shape of the pore with the copper binding sites. C-D-E) Cross sections of the trimer helix arrangement at the extracellular side. (C) in the middle of the bilayer (D) and at the intracellular side (E).

The methionines in the MXXXM motif, conserved in all Ctr proteins and located at the extracellular end of TMD2 (Fig. 2b and 3) reside in close apposition to each other.
Substitution of either of the two methionine residues in the MXXXM motif by alanine or serine residues abolishes yeast Ctr1 and human Ctr1 mediated copper transport activity, while conversion in cysteine or histidine residues does not significatively affect copper uptake (Puig S et al., 2002; Eisses and Kaplan, 2005b). It is likely that such motif participates in the formation of a copper binding site, which probably acts as a selective filter similar for the metal. A similar model was described for K-channels (Doyle DA et al., 1998).
Several lines of evidence suggest that binding of Cu to this motif may induce a conformational switch, and such switch could trigger internalization from plasma membrane since mutation of either methionine residues in the group abolishes hCtr1 clearance from cell surface following high extracellular copper concentration (Guo et al., 2004).
Each hCtr1 trimer contains two additional copper binding sites located at the opposite ends of the pore. One extracellular coordinated by the methionines in the MPM sequence in the N-terminal (Puig et al., 2002; Eisses and Kaplan 2005b), and one intracellular coordinated by the Cys HCH sequence in the C-terminal (Xiao et al., 2004; Wu et al., 2009).
The authors showed by inductive plasma-optical emission spectroscopy (ICPOES) coupled to X–ray spectroscopy that the hCtr1 trimer can simultaneously bind two Cu(I) through these three distinct binding sites and both ions are coordinated by three Cu-S thioether bounds (De Feo et al., 2009), typical of copper exchange reactions mediated by intracellular copper chaperones and their target (Davis and O'Halloran, 2008).
The authors propose a model where copper moves through the pore by exchange reactions between distinct binding sites and these reactions induce conformational switches (De Feo et al., 2009). Given the higher thermodynamic stability of Cu(I)-Cys coordination than the Cu(I)-Met coordination, the C-term intracellular copper binding site residues would provide a thermodynamic sink, allowing transport of copper in ATP independent way (Puig et al., 2002).
Other conserved residues have been studied by mutagenesis. His-139 is probably involved in interaction between monomers more than contributing to form a copper-binding site (Eissen and Kaplan, 2005b; De Feo et al., 2009). Methionines, in particular a MXXXM motive and His-rich regions in the N-terminal have been associated with high affinity transport (Puig et al., 2002).

1.2.2 Ctr1 transcriptional regulation

In yeast, the 5' regulatory regions of the CTR1, CTR3 and FRE1 genes contain a CuRE (Cu responsive element) element that is essential for transcriptional up-regulation in response to copper starvation and also for repression under conditions of copper excess (L'Abbe et al., 1998). The MAC1 (Metal-binding activator) transcription factor can bind to CuRE elements in copper transport pathway genes, modulating transcription in response to copper starvation (Yamaguchi-Iwai et al., 1997). Copper dependent transcriptional regulation in higher organisms is still controversial. Vertebrate do not code for a MAC1 homologue and hCtr1 mRNA levels do not seem to change as a function of copper state as reported for liver and intestinal mucosa of adult mouse (Lee et al., 2000) and intestinal human cells (Tennant and al., 2002; Bauerly et al., 2002).
So far in vertebrate copper dependent Ctr1 transcriptional regulation was reported in specimens of *Sparus aurata* exposed to copper. While dietary copper induced a decrease in trascriptional levels of expression of Ctr1 in the intestine and liver, waterborn copper exposure induced an increase Ctr1 mRNA levels in the intestine and the kidney (Minghetti et

al., 2007). The authors hypothesize that this differential regulation may be required in fish to cope with two different routes for copper acquisition in these animals.
Recently it was shown that the hCtr1 promoter contains three binding sites for transcription factor Sp1 (Sp1 transcription factor) and that zinc finger domain of Sp1 functions as a sensor of Cu that regulates hCtr1 transcription levels in response to Cu concentration variations (Song et al., 2008). The low magnitude of these changes in hCtr1 mRNA expression may explain why other studies failed in identifying variations in hCtr1 transcription levels in response to copper stress conditions.
Further studies will be required to verify if Sp1 can regulate in a coordinate way transcription of multiple genes involved in copper homeostasis and in particular Ctr2.
It will be important to address the mechanism by which Sp1 can sense variations in copper levels.

1.2.3 Ctr1 localization and trafficking

Most of the studies about hCtr1 steady state subcellular localization have been carried out in cell cultures, since the earlier works it has been reported that localization is dependent of the cell line studied. The protein can be observed either on the cell surface, in a perinuclear vesicular compartment, not yet identified, or on both (Klomp et al., 2002; Puig et al., 2002)
Studies carried out in Hela cells and Chinese Hamster Ovary (CHO) transfected with hCtr1, showed that even low extracellular copper concentration triggers a very rapid clearance from the plasma membrane through a clathrin-dependent endocytosis. At high extracellular copper concentrations hCtr1 degradation was observed as well (Petris et al., 2003). The same group later showed that while the conserved MXXXM in the second TMB domain is essential for both copper induced endocytosis and degradation, the MMMMPM motif in the extracellular domain near to the first TMB mediates endocytosis under low copper concentration (Guo et al., 2004). Other groups reported no change in endogenous Ctr1 localization followed by copper exposure (Klomp et al., 2002; Eisses et al., 2005a).
It is conceivable that copper-stimulated endocytosis of hCtr1 only occurs in certain cell types and that could also explain the different steady state localization but fewer studies are available about Ctr1 localization in vivo.
A different Ctr1 distribution in duodenal enterocytes was observed in adult compared with suckling mice, while the former had pronounced intracellular staining, the latter showed predominant apical staining (Kuo et al., 2006).
Ctr1 has been reported to re-localize on the plasma membrane in mammary gland cells in response to sucking and prolactin stimulation (Kelleher and Lönnerdal, 2006). These studies suggest that Ctr1 expression is modulate in response to copper status mainly by post-translational regulation, and in particular trafficking, rather than by transcriptional activation or repression.

1.2.4 Ctr1 post-translational modifications

Human Ctr1 has two glycosylation sites, both located in the amino terminus side of the protein. A N-linked oligosaccharide is added to residue Asn-15 in the consensus sequence NX[T/S] but the function of this glycosylation is still unknown, since mutagenesis of this residue and loss of the N-linked oligosaccharide does not seem to influence half time, cell surface exposure or Cu transport activity (Klomp et al., 2003; Maryon et al., 2007). The N-

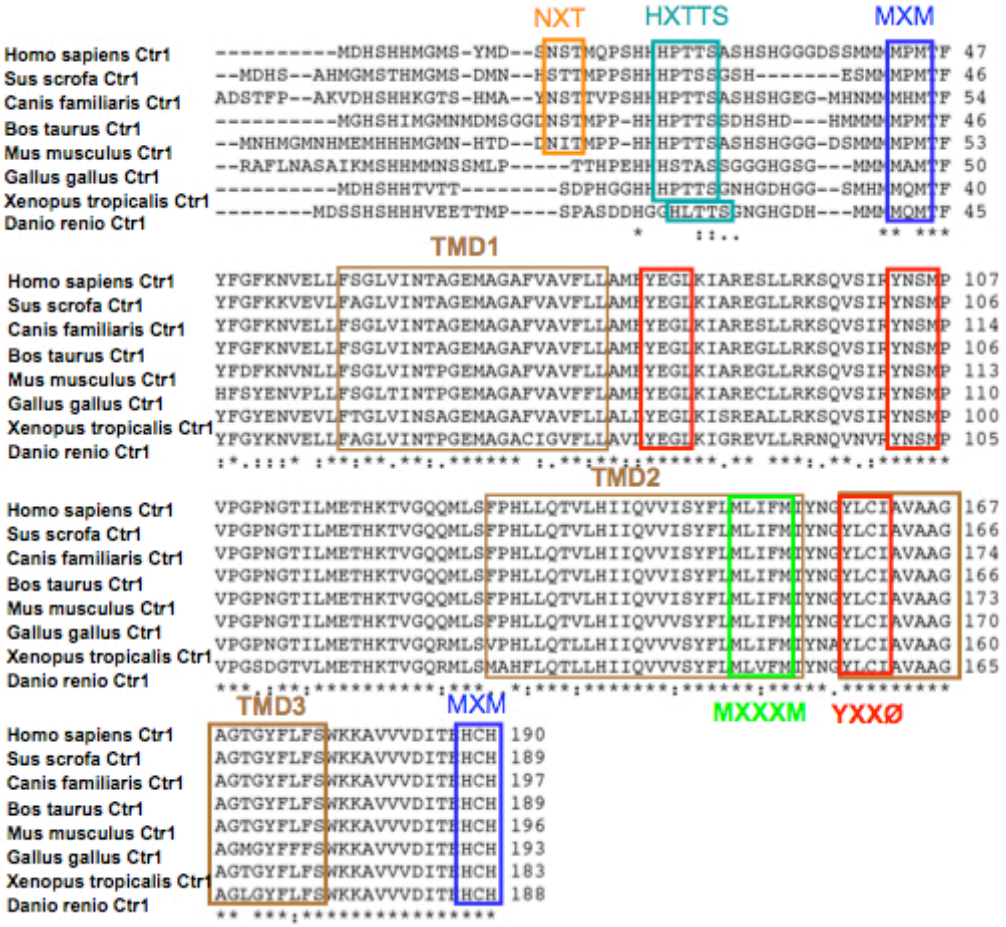

Figure 4. Sequence alignments of Ctr1 sequences from different vertebrate species using ClustalW. Predicted trasmembrane domains (TMD) are in brown. The putative transmembrane copper binding domain (MXXM) is in green, putative N-term and C-term copper binding domains (MXM) are in blue, and putative lysosomal sorting signals are in red. N-glycosylation site (NXT) is in orange and O-glycosylation site (HXTTS) is in cyan. Sequences were downloaded from UniProt (Universal Protein Resource www.uniprot.org).

glycosylation consensus sequence NX[T/S] seems highly conserved in mammals but not in other vertebrates (Fig. 4).

An O-linked oligosaccharide is added to the residue Thr-27, and seems important to proctect Ctr1 from proteolytic degradation. Chemical or genetic removal of this oligosaccharide results in the production of a cleaved form of hCtr1, of apparent molecular mass 17kDa, lacking of approximatively 30 aminoacids from the aminoterminus. This shorter form seems to retain about 50% of copper uptake in comparison to the full protein (Maryon et al., 2007).

It is currently unknown how this proteolytic cleavage is regulated, and if the full and the short form of hCtr1 localize to different compartments or have distinct functions.

The O-glycosylation site is part of an aminoacid array PT[T/]S that seems highly conserved in all vertebrate sequences (Fig. 4).

1.2.5 Ctr1 role in vertebrate development and physiology

Ctr1 has been shown to be essential for correct development in different vertebrate models. Ctr1 null mice die *in utero* during gestations and present severe development defects (Kuo et al., 2001; Lee et al., 2001).
Knockdown of *ctr1* by antisense morpholino oligonucleotides (MOs) causes early lethality in *Zebrafish larvae*, and in tissues where Ctr1 was most heavily expressed, in particular brain and spinal cord, an extensive cell death was observed (Mackenzie et al., 2004).
The similarity in the expression pattern in different vertebrate species could indicate that in early embryos Ctr1 is required at high levels in all cells.
A recent study highlighted the possibility that Ctr1 plays a role in regulation of stem cells differentiation and tissue morphogenesis during embryogenesis by physical interaction with tyrosine kinase Laloo involved in FGF activation pathway, independently by Ctr1 copper transport activity (Haremaki et al., 2007).
Generation of conditional Ctr1 knockout in intestinal epithelial cells suggested a role for Ctr1 in dietary copper uptake. Those mice exhibit striking growth defects and a concomitant copper deficiency in all peripheral tissues (Nose et al., 2006). The precise localization of mouse Ctr1 in intestinal epithelial cells is controversial, since different groups reported either apical (Nose et al., 2006; Kuo et al., 2006) or basolateral localization (Zimnika et al., 2007). Interestingly the Ctr1 null IECs (Intestinal Epithelial Cells) accumulate high levels of non bioavailable copper, probably trapped in intracellular compartment, suggesting a role for Ctr1 in intracellular copper mobilization more than in mediating Cu uptake from the intestinal lumen. Further studies will be required to decipher Ctr1 localization and mechanism of action in these cells.
Conditional hepatic Ctr1 knock out mice show lower copper concentrations in the liver and in blood compared to control animals, but do not have a pronounced copper deficiency in other tissues and have only mild growth defects (Kim et al., 2009). Interestingly in these transgenic mice while biliar copper excretion is reduced, more copper is secret in the urine, suggesting a coordinate role for liver and kidney in maintaining copper homeostasis in the body.

1.2.6 Copper Transporter 2 (Ctr2)

While much is known about the plasma membrane transporters, mediating copper uptake from the extracellular environment, very little information is available regarding intracellular copper transporters that have structural homology to the plasma membrane Ctr1 proteins.
Vacuolar copper transporters sharing sequence homology with Ctr family were firstly characterized in yeast *Saccharomyces cerevisiae* (Portnoy et al., 2002) and *Saccharomyces pombe* (Bellemare et al., 2002). In particular the former, designated as Ctr2, was shown to function in mobilizing vacuolar intracellular copper stores through a mechanism likely similar to that used by Ctr1 for copper import (Rees and Thiele, 2004).
Following studies in yeast supported the hypothesis that yeast Ctr2, as Ctr1, requires the presence of a metalloreductases to work properly, suggesting both proteins transport copper across membranes preferentially in the reduced form Cu(I) (Rees and Thiele, 2007). The recently identified family of metalloreductases in mammals, renamed STEAP, suggests the possibility that the reduction of Cu(II) to Cu(I) mediated by this protein is coordinated with Ctr2 activity (Ohgami et al., 2006).
A Ctr2-like protein, renamed hCtr2 was identified in humans and mice by sequence homology with hCtr1 (Zhou and Gitschier, 1997).

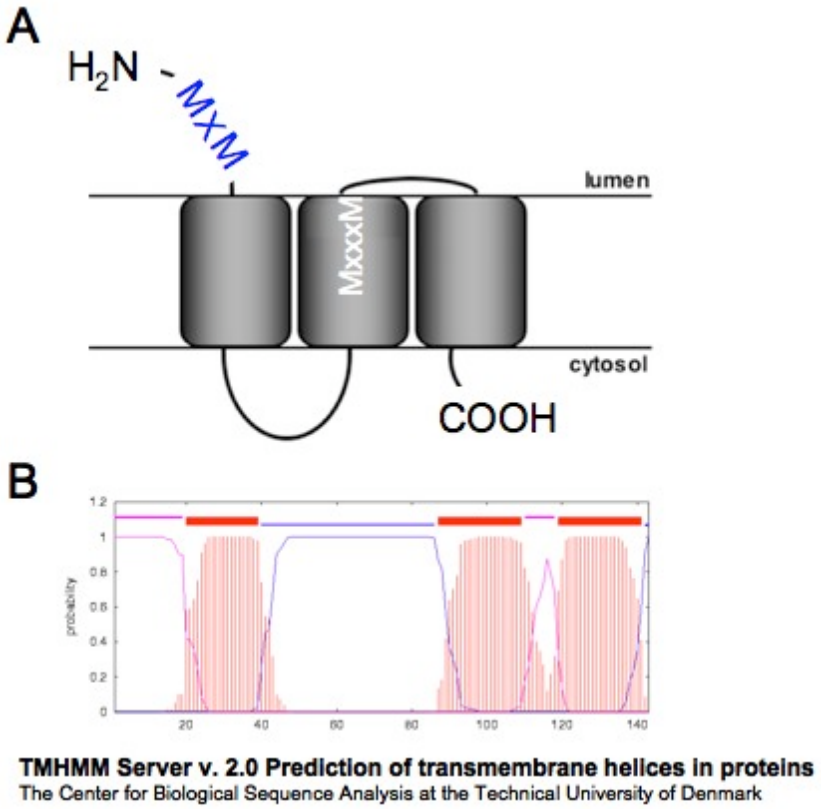

Figure 5. A) Ctr2 predicted topology based on sequence homology with Ctr1. The putative transmembrane copper binding domain (MXXM) is in white, and the putative N-term copper binding domain (MXM) is in blue. B) Hydrophobic plot of the mouse Ctr2 sequence highlighting the three predicted transmembrane domains.

No structural and topological data are available for hCtr2, but based on the prediction of the TMDs (Fig. 5B) and sequence homology with hCtr1, the N-terminus is predicted to be in the vesicular lumen, and the C-terminus and the loop between TMD1 and TMD2 in the intracellular side (Fig. 5A).

While the three TMDs share high homology with hCtr1 and the MXXXM and GXXXG motives are fully conserved, the N-terminus and C-terminus of hCtr2 are significantly different from hCtr1 (Fig. 6).

Notably hCtr2 lacks the His- ad Met- rich domains in the N-terminus that in hCtr1 have been associated with high affinity copper transport, and the putative copper binding site HCH in the C-terminus (De Feo et al., 2009) showed to be important for hCtr1 folding and holigomerization (Lee et al., 2007). Furthermore the N- and O-glycosilation sites conserved in all the hCtr1 sequence are missing in hCtr2 (Fig. 5) and western blot studies seem to confirm that hCtr2 is not glycosilated (van den Berghe et al. 2007, Bertinato et al., 2008).

van den Berghe et al. (2007) showed that overexpression of hCtr2 in human cells results in increase in bioavailable cytosolic copper only in presence of high extracellular copper concentrations, with a mechanism dependent of the integrity of the MXXXM motif.

Bertinato et al. reported similar result showing by kinetics studies that hCtr2 dependent increase in cellular total copper content was concentration dependent, saturable and not due to a decrease in copper excretion (Bertinato et al., 2008).

These studies suggested the hypothesis that hCtr2 mediates low affinity copper import in human cells.
Ctr2 localization remains more elusive, in fact while overexpressed hCtr2 epitope-tagged forms clearly co-localize with lysosomal markers (van den Berghe et al., 2007) endogenous hCtr2 seems to have a more diffuse perinuclear staining and was partially detected on the plasma membrane (Bertinato et al., 2008). It is possible that, as for hCtr1, also hCtr2 localization is cell specific.

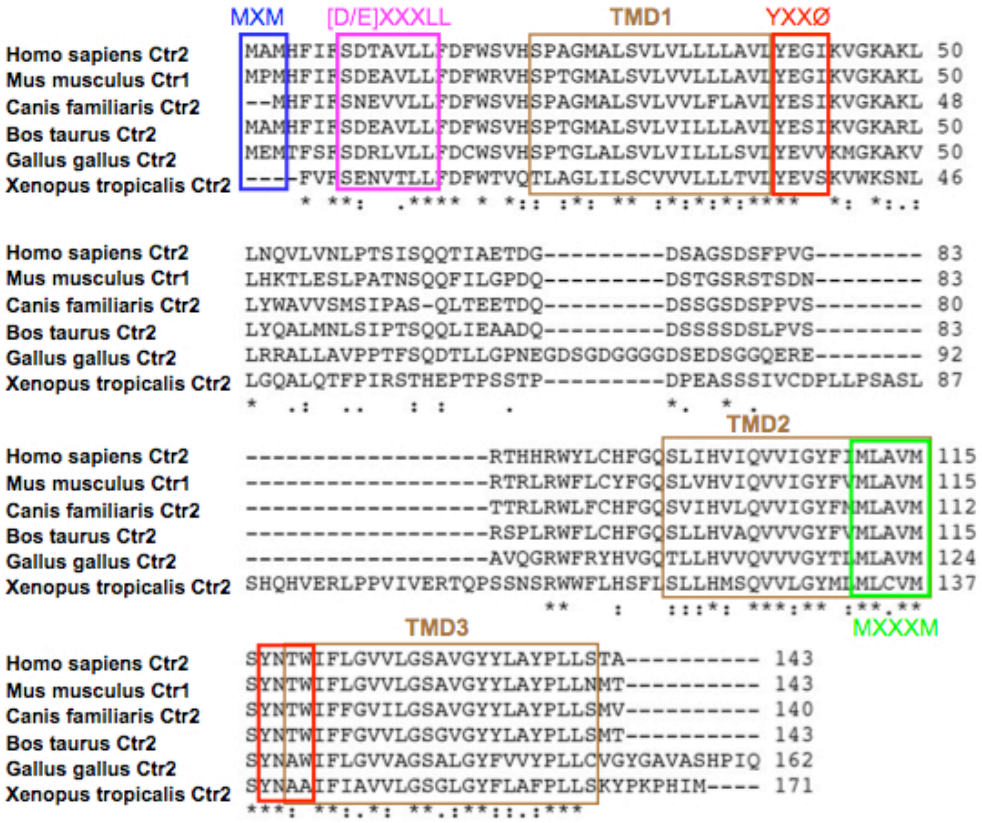

Figure 6. Sequence alignments of Ctr2 sequences from different vertebrate species using ClustalW. Predicted trasmembrane domains (TMDs) are in brown and indicated by roman numbers. The putative transmembrane copper binding domain (MXXM) is in green, putative N-term binding domain (MXM) are in blue, putative lysosomal sorting signal [D/E]XXXL[LI] in pink, and putative lysosomal sorting signal YXXØ are in red. Sequences were downloaded from UniProt (Universal Protein Resource www.uniprot.org).

1.2.7 Putative lysosomal sorting signals in Ctr1 and Ctr2 vertebrate sequence

Analysis of the vertebrate Ctr1 and Ctr2 sequences revealed the presence of three conserved putative YXXØ signals in both proteins and an additional D[E]XXXL[LI] motif in Ctr2 (Fig. 4 and 6). The position and number of these motives in the Ctr proteins are unusual (Bonifacino JS, personal communication), and only mutagenesis of these sequences will

allow verifying their putative involvement in either trafficking or degradation of Ctr1 and Ctr2 in the lysosomes.
These motives are conserved throughout the protist and animal kingdoms and in order to be active need to be exposed to the solvent being accessible to interactions with the sorting machinery. Given their close location to the putative TMDs it is not possible to predict if the YXXØ signals are accessible to the sorting machinery, or possibly they become closer only after the conformational changes induced by copper binding (De Feo et al., 2009).

1) D[E]XXXL[LI]: these dileucin sorting signals can either participate in internalization and degradation of surface receptors when following a serine residues (CD3 and CD4) or when constitutively active can contribute to lysosomal-endosomal localization of proteins and in the latter case are usually found in the C-terminus (NPC1 and LIMP2). These motives are conserved throughout the protist and animal kingdoms. Mutagenesis analysis revealed that the substitution of either leucin abrogates the function while the acid residues D/E favors lysosomal targeting but is less important for internalization. These signals are recognized by AP-1, AP-2 or AP-3 complexes (Bonifacino and Traub, 2003).
2) YXXØ: these tyrosine based sorting signals are found in a broad range of endocytic receptors (Transferrin receptor, cation dependent mannose phophate receptor, LAMP1, LAMP 2, among others) that have different intracellular localization but all share the property of trafficking to the plasma membrane to some extent. These signals have been implicated in several functions such as endocytosis, lysosomal targeting and basolateral targeting in polarized cells. Mutagenesis analysis revealed that the tyrosine is essential for function and when a glycine precedes the Y residue this motif is involved in lysosomal targeting. Usually residues in X positions tend to be acids while the Ø position accommodates residues with bulky hydrophobic side chains. Also the distance from transmembrane domains (TMD) affect the activity of the tyrosine based signal: purely endocytic YXXØ signals are usually found 10-40 residues from TMD and not at the C-terminus of proteins, while lysosomal targeting signal are located 6-9 residues from TMD and usually at the C-terminus of proteins. YXXØ signals have been shown to interact with the μ subunits of the four AP complexes, and this interaction may be regulated by phosphorylation of the YXXØ signals or adjacent residues (Bonifacino and Traub, 2003).

1.2.8 Aims of the research

The goal of the research was to study by immunoblot the expression of endogenous mouse Ctr2 (mCtr2) in cell cultures and in mouse models to understand its regulation, and to employ siRNA mediated silencing to get insights about its function in copper homeostasis.
We collected evidences about regulation of mCtr2 protein levels in a copper and Ctr1 dependent way. Our observations in cells and transgenic mice suggest that lack of Ctr1 induces a strong downregulation of Ctr2 probably by a post-translational mechanism.
The other goal was to inquire its subcellular localization and putative trafficking in response to copper status by indirect immunofluorescence.
We observed an exclusive intracellular localization in a perinuclear intracellular compartment and no co-localization with lysosomal markers.
Furthermore immunofluorescence experiments, supported by sequence analysis, suggest that lysosomes may play a role in mCtr2 biology not as resident compartment, but as a degradation site.

2. Materials and Methods

Reagents and antibodies

All chemical reagents were of molecular biology purity level. Anti mouse Ctr2 antibody (mCtr2Ab) was raised in rabbits: a synthetic peptide of the sequence H2N-VSIRYNSMPVPGPNGTILC-CO2H, which corresponds to the 19 aminoacids in the putative cytosolic loop between transmembrane domains 1 and 2 of mouse Ctr2 was used as antigen for generation and affinity purification of rabbit polyclonal antiserum by Bethyl Laboratories, Inc. (Montgomery, TX).
Anti human Ctr1 antibody (hCtr1Ab) was raised in rabbits: a synthetic peptide of the sequence H2N-VSIRYNSMPVPGPNGTILC-CO2H, which corresponds to the cytosolic loop between transmembrane domains1 and 2 of mouse and human Ctr1, was used as antigen for generation and affinity purification of rabbit polyclonal antiserum by Bethyl Laboratories, Inc. (Montgomery, TX).
Other antibodies used were commercially available: actin (Santa Cruz), GAPDH (Ambion), CCS (Santa Cruza), COXIV (Abcam), LAMP1 (eBioscience), RAB7 (Sigma), RAB9 (ABcam), PDI (Abcam), Cadherin (ABcam), 58k Golgi protein (Abcam).

Cell cultures

Several murine cell lines were used to study mCtr2 expression and localization: RAG (renal adenocarcinoma), Aml12 (normal liver hepatocytes), C_2C_{12} (myoblasts), 3T3 (embryonic fibroblasts). E1/E3 (wild type mouse embryonic fibroblast), E7/E8 (Ctr1 knockout embryonic fibroblast) were generated as described by Lee et al. (2002). Commercial cell lines were cultured in media recommended by ATCC (American Type Culture Collection). E1/E3/E7/E8 were cultured in Dulbecco's Modified Eagle's medium supplemented with 20% fetal bovine serum, 2mM glutamine, nonessential amino acids, 55μM 2-mercaptoethanol, 100 units/ml penicillin and streptomycin, 50 mg/liter of uridine and 110 mg/liter of pyruvate.

Copper exposure and copper chelation experiments

For copper exposure time course experiments RAG cells were incubated in a growth media containing copper chloride, $CuCl_2$ (Sigma) at final concentration 50 μM. Cells were harvested for protein extraction after 2h, 4h, 8h, 24h and 72h. Fresh media containing copper was changed every 24h. A pool of cells at the same confluence of the ones exposed to the copper containing media was harvested for protein extraction as a t0.
For copper chelation experiments E1/E8 cells were incubated in growth media containing BCS (Bathocuproine disulphonate) (Sigma) at final concentration 1mM and cells were harvested for protein extraction after 24h. A pool of cells grown in BCS free media were simultaneously grown and harvested for protein extraction at the same time.

RNAi transfection

siRNA (small interfering RNA) oligonucleotides targeting to either coding sequences or 3'UTR sequences of the mouse Ctr2 mRNA (1: 5' AAAGTAGCCAATTACCACCtg 3'; 2 GTATCCAGGTTCCATGGCCtt 3'; 3: TAAAATGACCTAGCTTTGGtt) and negative control siRNA oligonucleotides were designed and purchased from Ambion.
Cells at 50% confluence were transfected for 48h with INTERFERin (Polyplus Transfection) and siRNA oligos at final concentration of 30nM, according to manufacturer instructions.
For time course experiment non transfected cells, cells transfected with negative control siRNA and cells transfected with Ctr2 siRNA were grown simultaneously and harvested at the same time points. After transfection fresh media was added to the cells, and it was changed every 24h.

Generation of $Ctr1^{+/-}$ and $Ctr1^{int/int}$ mice

C57BL/6 male and female mice were used as wild types. Generation of Ctr1 heterozygous mice was described by Lee et al. (2001). Briefly a targeting vector containing a neomycin PGKneo gene expression cassette and 2.0kb and 3.5 kb genomic sequence flanking respectively exons 5' and 3' of Ctr1 gene was introduced into mouse derived embryonic stem (ES) cell line by electroporation. The thymidine kinase (*tk*) gene and neomycin resistance (*neo*) gene were used to select ES cells in which the targeting construct had integrated into the genome. Clones carrying the targeted *Ctr1* allele were injected into blastocysts collected from C57BL/6 mice following. The $Ctr1^{+/-}$ mice were generated by crossbreeding between male chimeric mice and female C57BL/6mice.
Generation of intestinal epithelial Ctr1 knockout mice ($Ctr1^{int/int}$) was described by Nose et al., 2006. Briefly the Ctr1 structural gene was flanked by loxP sites followed by the PGKneo gene cassette with an additional loxP site. The targeting vector was used to generate chimeric and heterozygous mice as described above. The PGKneo gene was removed by crossbreeding with EIIaCre mice, and mice having the desired allele of Ctr1 flanked by loxP ($Ctr1^{flox/flox}$) were obtained. The Ctr1-deleted allele was obtained by crossbreeding with Villin-Cre mice. As a control for expression studies were used tissues from Ctr1 floxed mice ($Ctr1^{flox/flox}$) of the same age and sex.

Tissue samples collection

Tissues (brain, heart, liver, kidney, testis) were dissected after perfusion with phosphate-buffered saline (pH 7.4; PBS), frozen in liquid nitrogen, and stored at −80°C until use. The small intestine was opened along the long axis, washed in ice-cold PBS, soaked in PBS containing 1.5mM EDTA and protease inhibitors at 4°C for 10 min with gentle agitation (Chen et al., 2003). After incubation the mesenchyme layer was removed, and intestinal epithelial cells were washed three times with ice-cold PBS plus protease inhibitors and recovered by centrifugation at 200 × g for 7 min.

Protein isolation and quantification

Total crude extracts (T) were prepared homogenizing cell pellets or tissues in 5-10 volumes of a lysis buffer containing 1% Triton-X 100, 0,1% SDS and 1mM EDTA and protease inhibitors in PBS pH 7,4. Homogenates were incubated on ice for 1h, followed by centrifugation at 16,000xg for 20min at 4°C, or 100,000xg for 1h at 4°C. The supernatants were used as total extracts (T).
Supernantant (S) and pellet (P) fractions were prepared homogenizing cells and tissues kept in ice with a polytron in 10 mM Tris (pH 7,4) homogenization buffer containing 250mM sucrose and 2mM EDTA and protease inhibitors (inhibitor cocktail from Roche and PMFS 1mM). Homogenates were initially centrifuged at 5000g for 10min and pellet was discarded. Supernatants were further centrifuged at 100000g for 1h at 4°C, and second supernatants were kept as such (S), while pellets were suspended in cell lysis buffer, incubated on ice for 1h, centrifuged at 100,000xg for 30min to remove undissolved debris and the supernatants were used as a pellet fraction (P).
Protein concentrations were measured by the BioRad Protein DC Assay kit (BioRad Laboratories, Hercules, CA) with bovine serum albumin (Pierce) as a standard.

Differential centrifugation

RAG cell pellets were homogenized with a Dounce Homogenizer in 10mM Tris (pH 7,4) buffer containing 250mM sucrose, 2mM EDTA and protease inhibitors (inhibitor cocktail from Roche and PMFS 1mM). Homogenates were initially centrifuged at 1000g for 5min and pellet was discarded to remove nuclei.
Supernatants were transferred in a new tube and centrifuged at 3,000g for 10min at 4°C. Pellets were suspended in cell lysis buffer, incubated on ice for 30min, centrifuged at 16,000xg for 20min to remove undissolved debris and the supernatants were used as heavy mitochondrial fractions.
Supernatants were transferred in a new tube and centrifuged at 16,000g for 20min at 4°C. Pellets were suspended in cell lysis buffer, incubated on ice for 30min, centrifuged at 16,000xg for 20min to remove undissolved debris and the supernatants were used as light mitochondrial fractions.
Supernatants were transferred in a new tube and centrifuged at 100,000xg for 1h at 4°C.
Pellets were suspended in cell lysis buffer, incubated on ice for 30min, centrifuged at 16,000xg for 20min to remove undissolved debris and the supernatants were used as microsomal fractions. Last supernatants were kept as such (S).

Electrophoresis and western blotting

Protein extracts were resuspended in a 4X SDS-PAGE loading buffer for 10min with and without boiling at 95°C for 5min before loading into the gel. Isoproteic amounts were loaded into SDS polyacrylamide gel electrophoresis (SDS-PAGE) using Criterion Precast gradient gels either 8-16% or 10-20% (BioRad). Proteins were transferred from the gel to a PVDF membrane (BioRad) using a discontinuous buffer in a semi dry cell. Briefly, filter paper and membrane on the anode were soaked in Tris-CAPS buffer plus 15% methanol (60 mM Tris base, 40 mM CAPS, 15% MeOH, ph 9.6) while gel and the filter paper on the cathode was soaked in and Tris-CAPS plus 0.1% SDS (60 mM Tris base, 40 mM CAPS, 0.1 % SDS, ph

9.6). Transfer was performed at constant current 1.5mA per square centimeter of gel (for example, 120mA for a small 8 x 10 cm gel).
The membranes were blocked in 5% (w/v) non-fat dried milk in T-BST (25mM Tris/HCl, pH 7.4, 137 mM NaCl and 2.7 mM KCl, 0.05% Tween 20), incubated for 1 or 2h with 1:1,000 primary antibody dilutions, washed 3 times for 5min in TBS-T, incubated 1h with 1:5,000–1:10,000 HRP-linked secondary antibodies, washed 3 to 4 times for 5min in TBS-T and finally for detection the SuperSignal West Pico Chemiluminescent substrate kit (Pierce, Rockford, IL) and Denville Blue Bio Films (Denville Scientific, Metuchen, NJ) were used.

Indirect immunofluorescence microscopy

Cells grown overnight on coverslip were rinsed with ice cold PBS and fixed/permeabilized with two different methods.
In the first cells were fixed with 3.5% (w/v) paraformaldehyde in PBS pH7 for 10min, washed with 100mM glycine in PBS pH7, permeabilized with Triton-X 0.1% in PBS pH7 for 5 min and blocked for 30 min at room temperature with 1% (w/v) non-fat dried milk in PBS pH7.
In the second method cells were fixed with 100% MeOH at -20°C for 5min, and blocked for 30min at room temperature with 1% (w/v) non-fat dried milk and saponin 0.3% (w/v) in PBS pH7.
Cells were incubated for 2h at room temperature with primary antibody solutions in the blocking buffer at final concentration of 1:200 for 2h at room temperature, washed with PBS and incubated for 1h at room temperature in the dark with secondary solutions of AlexFluor (either 488 or 568) conjugated antibodies (Molecular Probes/Invitrogen) at final concentration 1:500.
Coverslips were washed several times in PBS mounted on coverslides using Prolong Antifade Kit (Molecular Probes/Invitrogen) and visualized with Axio Imager widefield fluorescence microscope (Carl Zeiss).

3. Results

3.1 Ctr2 expression in mouse cell lines

Initially different mouse cell lines (in particular Tm4, Aml12, C_2C_{12} and RAG) were tested to study mouse Ctr2 expression. Among these RAG cell line was selected as model for following characterization experiments, since it showed the highest Ctr2 expression levels. In particular this cell line was the only one where the putative Ctr2 monomeric form, whose apparent molecular weight matched the expected mouse Ctr2 size of 15 kDa, was easily detected in crude total extracts (Fig. 1, lane 1).

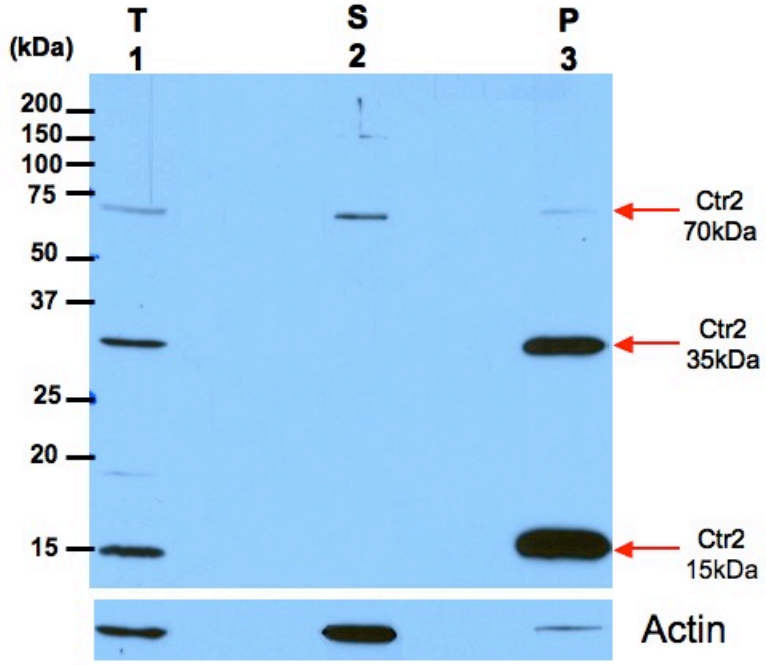

Figure 1. Representative western blot of RAG (T), supernatant (S) and pellet (P) protein extracts obtained from RAG cell line. The main bands detected with Ctr2Ab are indicated with red arrows. Membranes were stripped and reprobed for GAPDH. Molecular masses are indicated in kDa.

Usually 3 major bands were detected with the mouse Ctr2Ab in protein extracts from mouse tissues and mouse cell lines:

1) A 35kDa band strongly detected in all mouse cell lines and tissues
2) A 15kDa band, easily detected in total crude extracts of RAG cells, is also detected in other cell lines and tissues only in pellet extracts (Fig. 1, lane 3; Fig. 1A, lanes 1-2; Fig. 1C lanes 7-8) or in crude extracts prepared spinning at 100000g (Fig. 9, lanes 3-7). The molecular weight of this protein corresponds to the expected size of the primary translation product of mammalian Ctr2.
3) A 70kDa band not always detected.

Other bands, in particular 100kDa and 20kDa were only occasionally detected and their intensity was significantly lower than the ones described above.
Figure 1 shows a representative sub-cellular fractionation experiment using RAG protein extracts. After homogenization in a free detergent buffer and centrifugation at 100000g the 35kDa and the 15kDa bands are almost exclusively detected in the pellet fraction (Fig. 1, lane 3), containing membrane associated proteins, while the 70kDa is mainly but not exclusively observed in the supernatant (Fig. 1, lane 2), containing soluble proteins. Interestingly the intensity ratio between the 15kDa and the 35kDa bands is inverted from total to the pellet extract (Fig. 1, lanes 1 and 3). Actin, used as control is mainly retained in the supernatant, even though a small fraction is detected in the pellet.

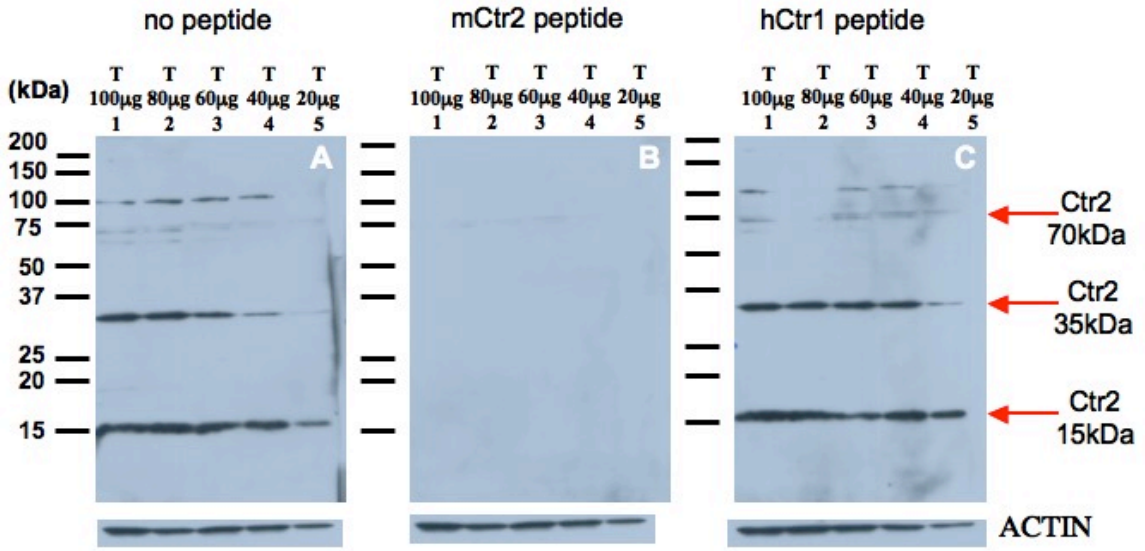

Figure 2. Antibody-peptide competition assay. Decreasing amounts (100÷20 µg) of RAG total extracts were loaded in triplicate on the same gel, proteins were blotted on a PVDF membrane, and 3 single identical membranes (A, B and C) were made. Membrane A was probe with a primary solution containing only anti-mCtr2 antibody, membrane B and C with primary solutions pre-incubated with 80M excess respectively of mCtr2 peptide and a hCtr1 peptide. The main bands detected with Ctr2Ab are indicated with red arrows. Membranes were stripped and reprobed for actin. Molecular masses are indicated in kDa.

In order to test the specificity of the antibody it was carried out an antibody-peptide competition assay. As shown in Figure 2, incubation of the mCtr2Ab with the peptide used as immunogen determines a lack of reactivity of the antibody towards the three main bands, while it is still possible to see some faint high molecular weight bands (Fig. 2B). In contrast, incubation of the Ctr2Ab with the same molar excess of a heterologous peptide, corresponding to the C-tail of hCtr1, it doesn't affect the detection of these proteins (Fig. 2C) and the blot is identical to the one obtained using a primary solution containing only the antibody (Fig. 2A). Actin used as a control indicates that all three membranes were equally loaded.

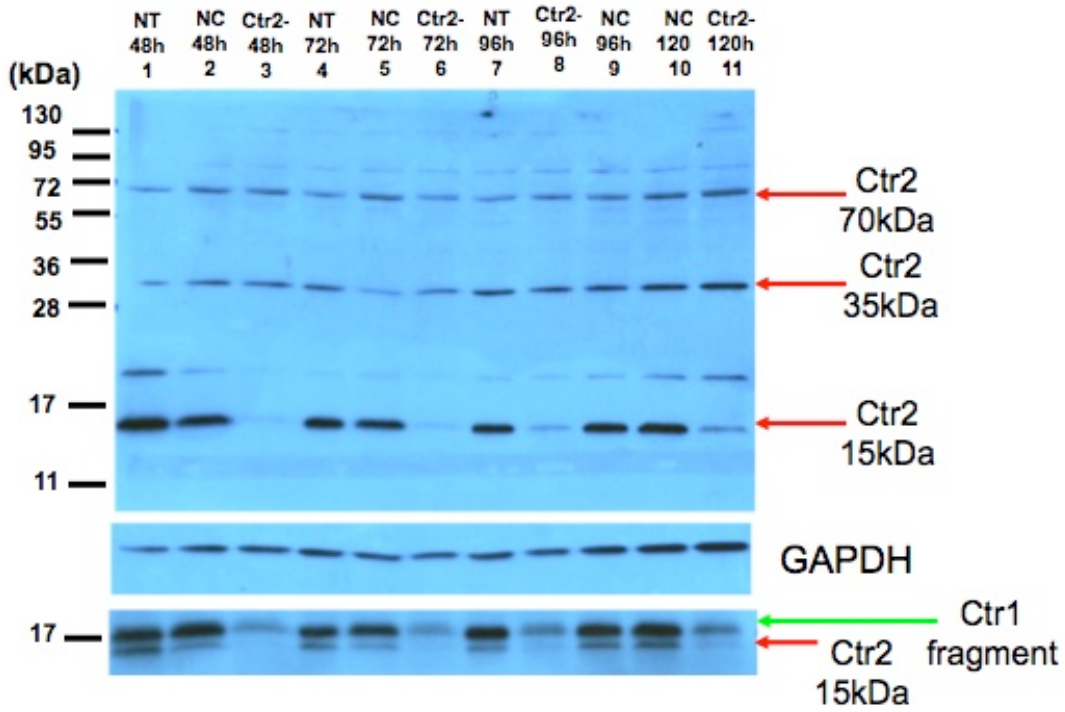

Figure 3. RAG total protein extracts after RNAi time course experiment. RAG cells at the same confluence were transfected with either Ctr2 RNAi oligos (lanes 3,6,8 and 11) or a negative control (NC) RNAi oligo (lane 2,5,9 and 10). Cells were harvested and proteins were extracted at 48h, 72h, 96h and 120h from the beginning of the transfection. For each time point non-transfected (NT) RAG cells at the same confluence were harvested and protein extracted. Main bands detected with Ctr2Ab are indicated with red arrows. Membrane was stripped and re-probed for GAPDH and Ctr1. Molecular masses are indicated in kDa.

To further test that the proteins recognized by the antibody were actually products of the Ctr2 gene, RAG cells were transfected with three siRNA oligos targeting either exon number 3 or the 3' UTR of the Ctr2 mRNA. Time course experiments were performed in order to verify the RNAi oligos efficiency in silencing the target proteins and also the duration of such effect. The combination of the three siRNA oligos induced a very efficient and repeatable knockdown of the 15kDa protein with a single transfection.

The silencing started from 48h after beginning of transfection (Fig. 3, lane 3), and lasted almost 5 days, (Fig.3 lane 11), even though at day 4 and 5 (Fig.3 lane 8 and 11) protein levels were rising back up towards control levels. No difference in 15kDa levels were observed at any time points between untreated cells and cells transfected with negative control RNAi oligo (Fig 3., lane 1 and 2; lane 4 and 5; lane 7 and 9).

The Ctr2 targeting RNAi oligos did not affect at any time point the levels of the 3kDa and 70kDa proteins, which remained undistinguishable from the untreated and negative control cells (Fig. 3). None of the three bands seem to significantly vary during the time course. GAPDH shows equal loading in each lane.

The same membrane blotted with a Ctr1Ab revealed that also the major band detected with this antibody, whose apparent molecular weight is 17kDa, was subjected to a knockdown in a time dependent manner very similar to the Ctr2 15kDa band (Fig. 5, lanes 3,6,8 and 11). The stripping procedure probably did not remove completely the Ctr2Ab off the membrane, and

the Ctr1 blot allows verifying that Ctr2 15kDa and the Ctr1 17kDa are two discrete and different proteins.

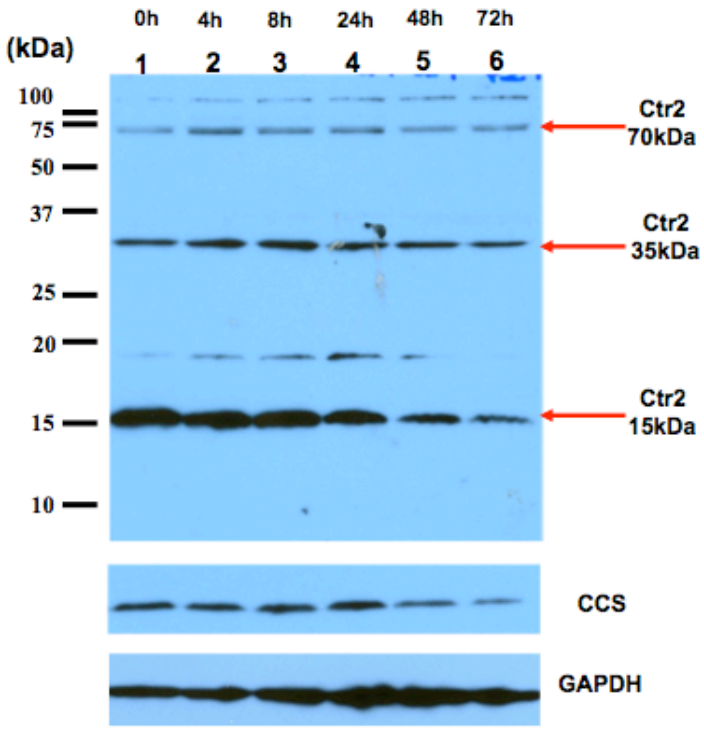

Figure 4. RAG total protein extracts after copper exposure time course. RAG cells were grown in MEM media containing 50μM of copper ($CuCl_2$). Cells were harvested and proteins extracted at different time points (0, 4h, 8h, 24h, 48h and 72h). Main bands detected with Ctr2Ab are indicated with red arrows. Membrane was stripped and re-probed for GAPDH and Ctr1. Molecular masses are indicated in kDa.

The effect of the addition of 50 μM $CuCl_2$ to the RAG cell culture media on Ctr2 protein expression was also tested. Extra copper in the media induced a time-dependent down-regulation of the 15kDa band, starting after 24h (Fig. 4, lane 4) and becoming more intense at 48h (Fig. 4, lane 5) and 72h (Fig. 4, lane 6), while the 35kDa and the 70kDa levels remained unaltered (Fig. 8).
Probing the same membrane for CCS (Copper Chaperone for SOD1) showed a decrease in the expression of this protein upon copper addition, with a time dependency similar to the one affecting the Ctr2 15 kDa protein (Fig. 8). GAPDH levels showed an equal loading of all samples.
Even after 72h of exposure to 50 μM $CuCl_2$ RAG cells did not show any morphological sign of toxicity.

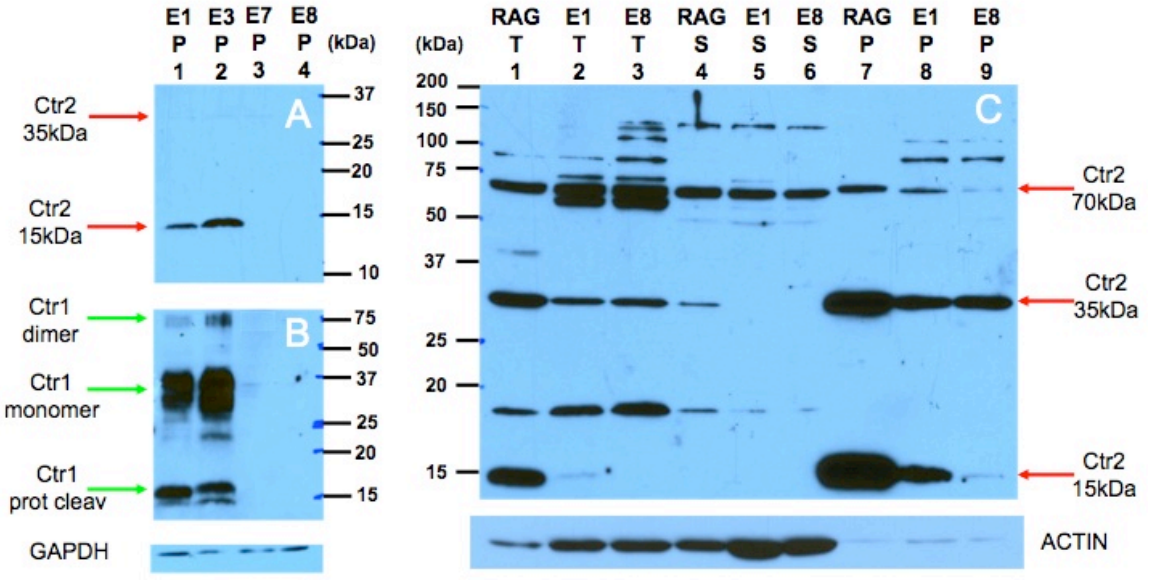

Figure 5. Ctr2 expression in wild type (E1, E3) and Ctr1 null (E7, E8) cell lines. A) Pellet extracts from E1, E3, E7 and E8 were probed with mCtr2Ab. Main bands detected with Ctr2 antibody are indicated with red arrows. B) The same blot was stripped and re-probed for Ctr1. Main bands detected with Ctr1 antibody are indicated with green arrows. Blot was stripped once more and re-probed for GAPDH. C) Western blot with total protein extract (T) (lanes 1,2,3) supernatant extracts (S) (lanes 3,4,5) and pellet extracts (P) (lane 7,8,9) respectively from RAG, E1 and E8 cell lines. Main bands detected with Ctr2Ab are indicated with red arrows. Membranes were stripped and re-probed for actin. Molecular masses are indicated in kDa.

It was decided to investigate Ctr2 expression levels in two embryonic cell lines previously generated and characterized in the laboratory, called E7 and E8, derived from Ctr1 null mouse embryos. As comparison we used two other cell lines, called E3 and E8, derived from wild type mouse embryos of the same age.

Figure 5A shows Ctr2 expression in pellet extract from E1, E3, E7 and E8. The 15kDa band is clearly detected in the two wild type cell lines but not in the Ctr1 null derived lines. The 35kDa is barely visible but is present in all 4 lanes while the 70kDa band was not detected in this blot. Re-probing the same membrane for Ctr1 confirmed that all the Ctr1 species (monomeric, dimeric and fragment) were detected only in the wild type cells (Fig. 5B). GAPDH was used as loading control.

Figure 5C shows a sub-cellular fractionation experiment carried out in RAG, E1 and E8 cells. As previously showed in all three cell lines 35kDa and the 15kDa bands are almost exclusively detected in the pellet fraction (Fig 1. lane 3), while the 70 kDa is retained mainly but not exclusively in the supernatant. In general E1 and E8 showed a lower expression of the 15kDa and 35kDa proteins compared to RAG cells. The 35kDa levels are basically identical in the two mouse embryonic cell lines, both in total extract (Fig. 5C, lanes 1-3) and pellet (Fig. 5C 7-9). Instead, the 15kDa has a markedly reduced expression in the E8 compared to E1. Overexposure of this blot was necessary to show that in E8 pellet the 15kDa band is still detectable, and therefore its expression is only strongly reduced and not completely suppressed (Fig. 5C, lane 9). 70kDa protein levels appear similar in all three cell lines. Blot overexposure resulted also in the detection of more bands especially at high molecular weight.

As previously shown in all cell lines extracts the intensity ratio between the 15kDa and the 35kDa bands is inverted from total to pellet extracts (Fig. 5C, lanes 1 and 7, 2 and 8).
Probing for actin showed an equal loading of the E1 and E8 total, supernatant and pellet extracts and lower levels of this protein in the RAG cells compared to E1 and E8. Similar results were obtained with E3 and E7 (data not shown).

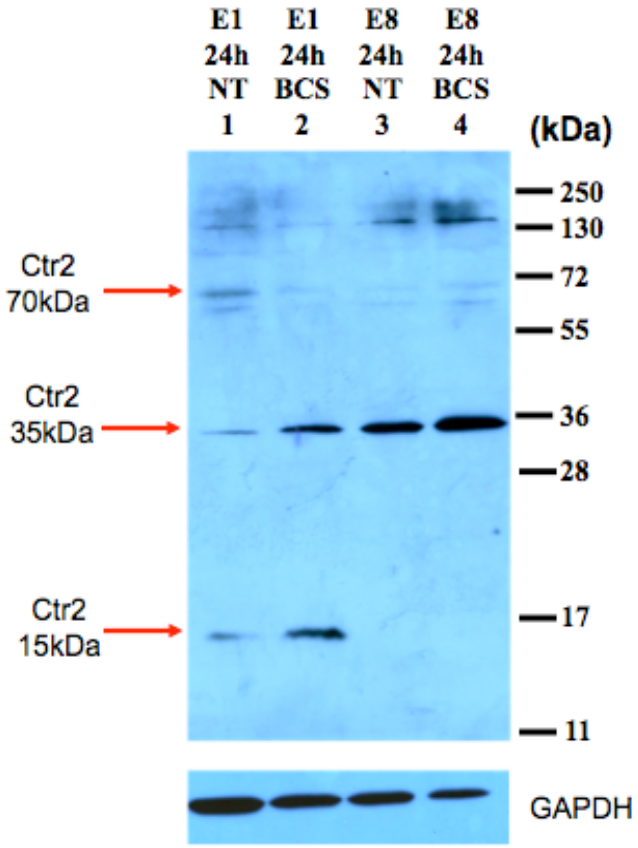

Figure 6. Effect of copper chelation on Ctr2 expression in E1 and E8 cells. For both lines controls and BCS treated cells were harvested at the same confluence and protein was extracted. Main bands detected with Ctr2Ab are indicated with red arrows. Membrane was stripped and re-probed for actin. Molecular masses are indicated in kDa.

The effect of copper chelation in wild type and Ctr1 null cell lines was analyzed after 24 hours of treatment. The copper chelator BCS (Bathocuproine disulphonate) induced an increase in 35kDa protein in both E1 (Fig.6 lane 1 and 2) and E8 (Fig. 6, lane 3 and 4) cells, and an increase of the 15kDa protein in E1 cells (Fig. 6, lane 1 and 2). The 15kDa band remained undetected in the total extracts of control as of BCS treated E8 cells (Fig. 6, lane 3 and 4). Probing for GAPDH indicates equal loading.
Centrifugation experiments in RAG cells were carried out differential in order to get information about Ctr2 subcellular localization. Four different protein extracts were generated from two different cell pool using sequential and increasing centrifugation speeds: 3000g (light mitochondrial fraction), 16000g (heavy mitochondrial fraction), 100000g (microsomal fraction) and the supernatant (S) generated from the last centrifugation.
The result of this experiment, shown in Figure 7, highlights a different centrifugation pattern for the two main proteins detected by the Ctr2Ab. The 15kDa band is present at comparable

levels in the heavy mithocondrial/3000g (Fig. 7, lane 1 and 2) and microsomal /100000g (Fig. 7, lanes 5 and 6) fractions, and it is slightly elevated in the light mitochondrial (160000g) fraction. Despite the blot was overexposed the 15kDa it is not detectable in the supernatant (Fig. 7, lane 7 and 8). Instead the 35kDa band is mainly retained in the light (3000g) and heavy mitochondrial fractions (Fig. 7, lane 1, 2, 3, 4), while it is markedly reduced but still detectable in the microsomal fraction (Fig 7, lanes 5 and 6) and in the supernatant (Fig. 7, lane 7 and 8). The amount of the 70kDa band seems to decrease from the first to the last fraction but is not clearly detected in this blot.
Among the other protein tested on the same fractions, GAPDH is mainly detected in the supernatant, COXIV exclusively in the mitochondrial fractions (mainly in the heavy), while the RAB7, a membrane associated protein and LAMP1, an integral membrane protein, showed a distribution pattern similar to the 15kDa band, with basically no signal in the supernatant. The same blot was also probed for Ctr1, and probably due to the multiple stripping and re-probing operations it was possible to clearly detect only the 17kDa band, whose distribution pattern was identical to the Ctr2, 15kDa protein (Fig. 7).

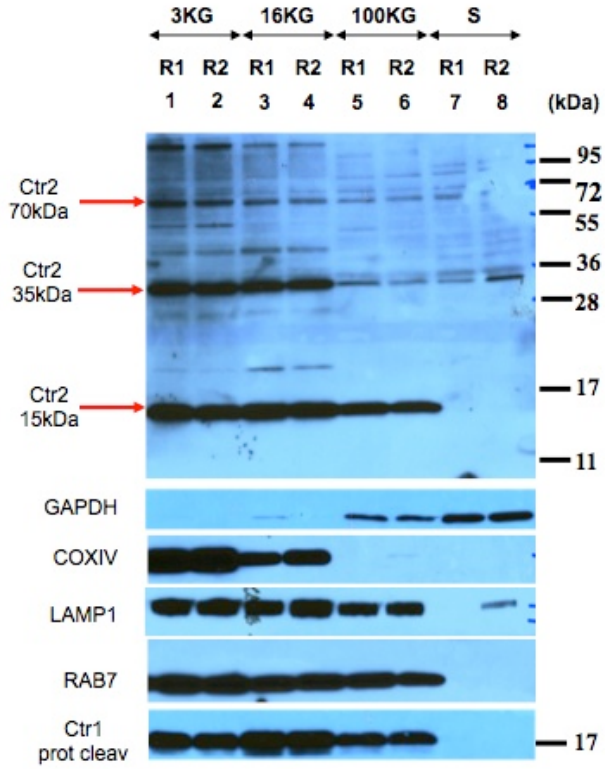

Figure 7. Differential centrifugation experiment using cell protein extracts from two different RAG cell pools (named R1 and R2). Cells were homogenized in detergent free buffer and the resulting homogenate was subjected to sequential centrifugations at increasing speed. After each centrifugation the pellet was resuspended in cell lysis buffer and supernatant was used for the following centrifugation. Main bands detected with Ctr2Ab are indicated with red arrows. Membrane was stripped and re-probed for GAPDH, COXIV, LAMP1, RAB7, and Ctr1. Molecular masses are indicated in kDa.

Ctr2 expression in mouse tissues

We investigated the expression of endogenous Ctr2 in tissues of wild type and transgenic mice fed on nutritionally complete diets.

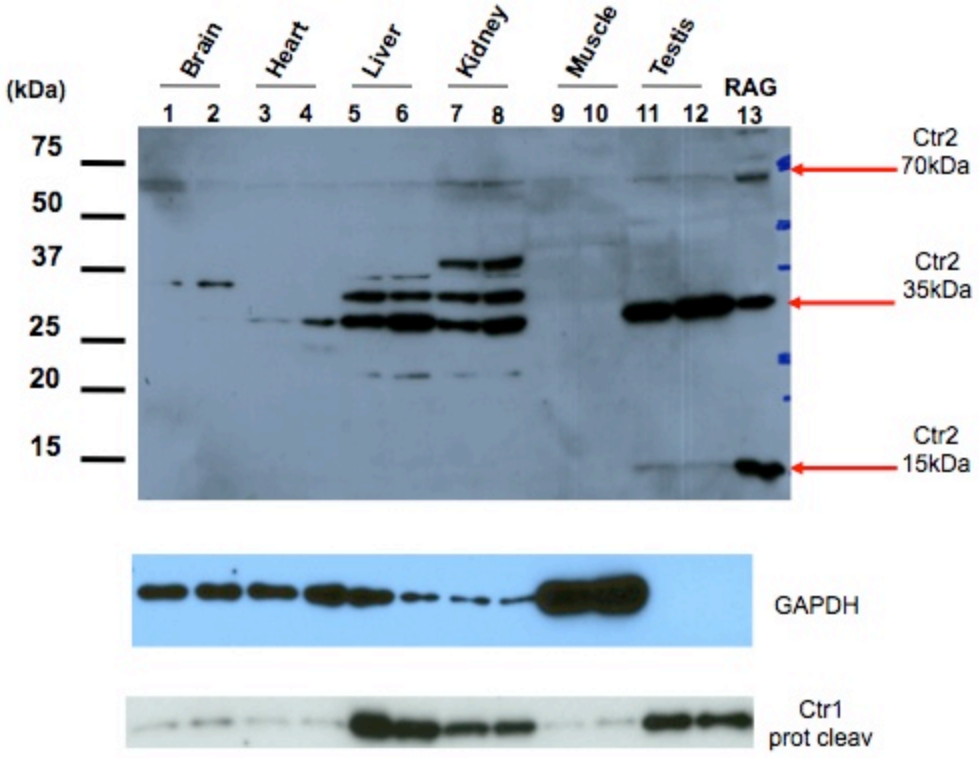

Figure 8. Representative western blot of total protein extracts from tissues of two wild type mice. Main bands detected with Ctr2Ab are indicated with red arrows. Membrane was stripped and re-probed for GAPDH and Ctr1. Molecular masses are indicated in kDa.

In general it was noticed that using the classic 16000g centrifugation speed for crude/total protein extract preparation, the 35 kDa band was relatively easy to detect, while it was much harder to detect the 15 kDa protein. The representative blot of tissue protein extracts from two different male wild type adult mice is shown in Fig. 8. A total protein extract from RAG cells was loaded in the gel to verify that the identity of the bands observed in tissues was the same of the ones detected in cell lines (Fig. 8, lane 13).
35 kDa protein expression appeared to be more robust in testis, occasionally in this tissue was also possible to detect the 15kDa band, usually after overexposure of the blot (Fig. 8, lanes 11 and 12). Liver (fig. 8, lanes 5 and 6) and kidney (fig. 8, lanes 7 and 8) also expressed high protein levels, even if lower than testis, brain (fig. 8, lanes 1 and 2) and heart (fig. 8, lanes 3 and 4) showed lower expression levels, while the muscle did not seem to express it at all (fig. 8, lanes 9 and 10). The 70 kDa band had a very low intensity in this blot.
In tissues we detected new bands not found in cell lines, in most cases these bands didn't have a regular and repeatable pattern, with the exception of two strong bands, of apparent molecular weight of 36 and 38 kDa expressed mainly in kidney and liver (fig. 8, lanes 5-8).

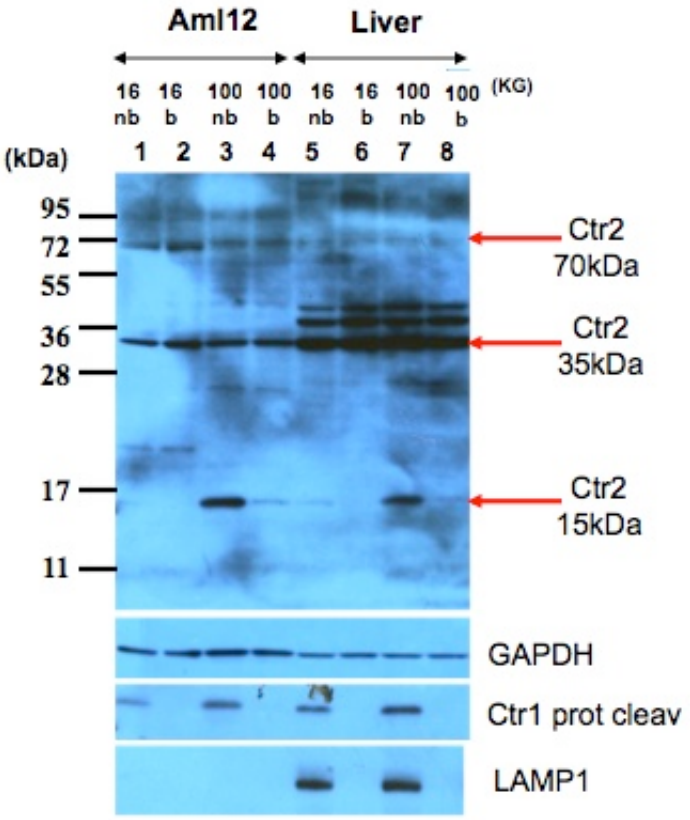

Figure 9. Effect of spinning speed and sample heating on Ctr2 protein detection. One Aml12 pellet and one liver sample were ressuspended in cell lysis buffer. From each suspension two aliquots of the same volume were spun at either 16000g (lanes 1,2,5,6) or 100000g (lanes 3,4,7,8). Isoproteic volumes of the resulting supernatant were loaded as such (lanes 1,3,5,7 marked as nb) or boiled for 5 min at 95°C before loading (lanes 2,4,6,8 marked as b). Main bands detected with Ctr2Ab are indicated with red arrows. Membrane was stripped and re-probed for GAPDH, Ctr1 and LAMP1. Molecular masses are indicated in kDa.

Given the results obtained by biochemical fractionation it was decided to test if the centrifugation speed after homogenizations of the pellets in the lysis buffer would affect the detection of the 15kDa protein.

To test this hypothesis we carried out a simple experiment: a cellular pellet from Aml12 (Fig. 9, lanes 1-4) and a piece of liver from a male adult mouse (Fig. 9, lanes 5-8) were homogenized in cell lysis buffer and splitted in 2 aliquots of equal volume. One aliquot was spun 16kg and the other at 100kg. The resulting supernatants were loaded on the gel in isoproteic amounts.

We found that in supernatants (either from cell or tissue) prepared spinning the homogenates at 100000g the detection of the 15kDa band by immunoblot resulted significantly enhanced, while the increased speed had no effect on the detection of 35kDa band (Fig. 9, lanes 3 and 7). In the same experiment Ctr1 17kDa fragment detection was improved in a similar but less marked way, while LAMP1 detection, found only in liver extracts (Fig. 9, lanes 3 and 7), was not affected by the spinning speed.

Furthermore boiling the samples prior to loading on the gel resulted in strong decrease in the intensity of the Ctr2 15kDa (Fig. 9, lanes 3-4 and 7-8), Ctr1 fragment (Fig. 9, lanes 1-2, 3-4,

5-6 and 7-8) and LAMP1 (Fig. 9, 5-6 and 7-8), but had no effect on the detection of Ctr2 35kDa band.
For the following experiments a 100000g spinning speed was employed in the preparation of total protein extracts from tissues.

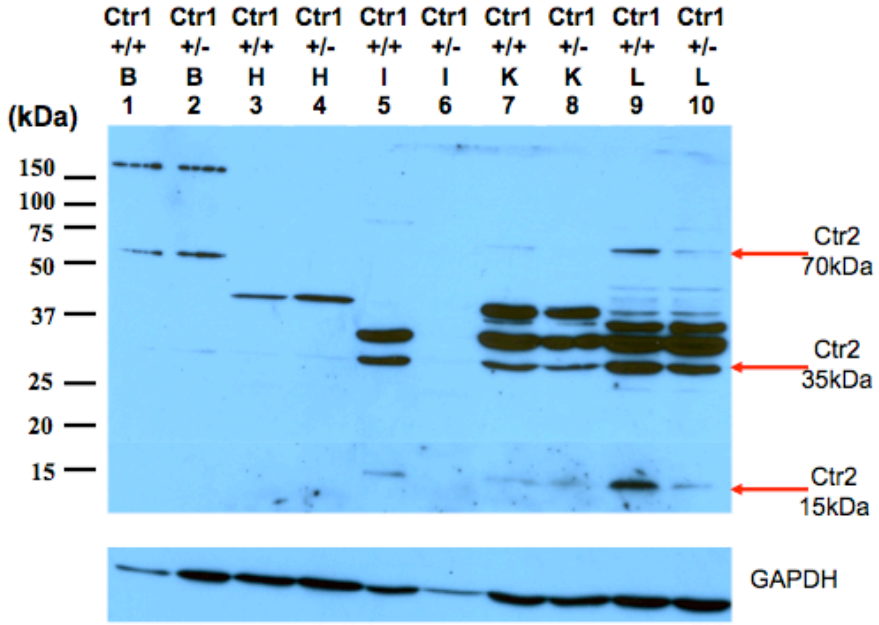

Figure 10. Ctr2 expression in brain (B), heart (H), intestine (I), kidney (K) and liver (L) of one control ($Ctr1^{+/+}$) and one heterozygous Ctr1 ($Ctr1^{+/-}$) adult mouse. Main bands detected with Ctr2Ab are indicated with red arrows. Membrane was stripped and re-probed for GAPDH. Molecular masses are indicated in kDa.

Then Ctr2 levels were tested in transgenic mice carrying only one copy of the CTR1 gene ($Ctr1^{+/-}$ heterozygous). Figure 10 shows a representative blot containing total protein extracts from different tissues of one adult wild type ($Ctr1^{+/+}$) mouse (Fig. 10, odd lanes) and one Ctr1 heterozygous ($Ctr1^{+/-}$) mouse, both female and of the same age. We observed in several samples that Ctr2 15kDa expression in the liver was significantly lower in $Ctr1^{+/-}$ (Fig. 10, lane 10) compared to $Ctr1^{+/+}$ (Fig. 10, lane 9). In this blot also the 70kDa seems to be regulated in a similar way.
Ctr2 15kDa was detected at low intensity in intestine and kidney (Fig. 9, lanes 5,7 and 8) but not in brain and heart, where high molecular bands were observed for both genotypes (Fig. 9, lanes 1-4).
GAPDH was used as loading control between same tissues: the intestinal sample from the heterozygous mouse was either underloaded or degraded (Fig. 9, lanes 1-4).

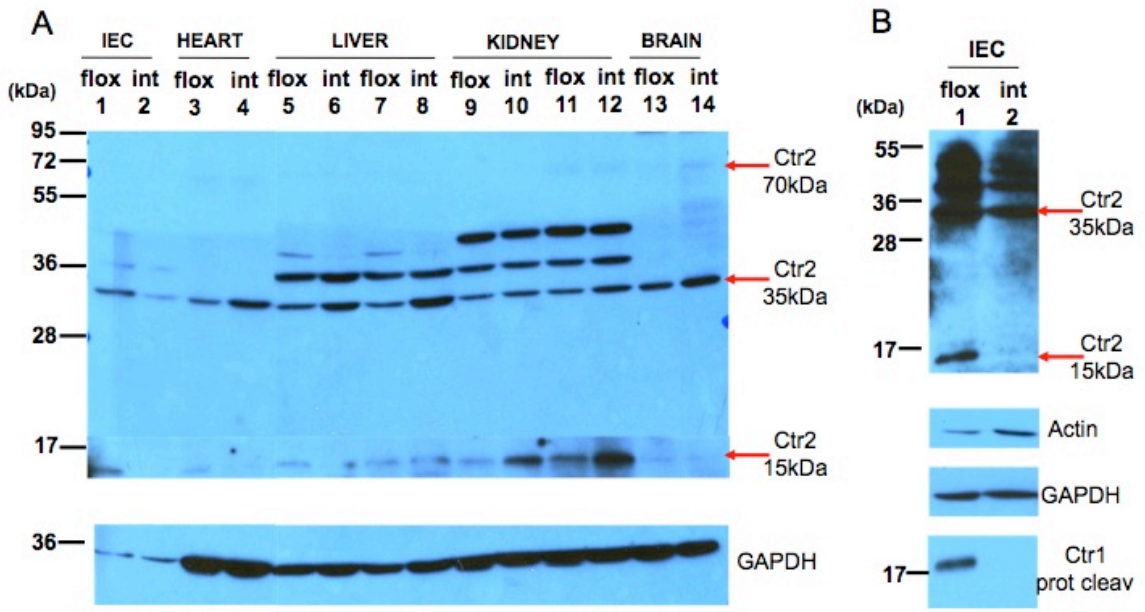

Figure 11. Ctr2 expression in control (flox) and intestinal conditional Ctr1 knockout mice (int). A) Ctr2 expression in intestinal epithelial cells (IEC), heart (H), and brain (B) of one control (flox) and in one intestinal conditional Ctr1 knockout (int) mouse. Ctr2 expression in liver (L) and kidney (K) of two control (flox) and two intestinal Ctr1 knockout (int) mice. Main bands detected with Ctr2Ab are indicated with red arrows. Membrane was stripped and re-probed for GAPDH. B) Ctr2 expression in intestinal epithelial cells (IEC) in one control (flox) and one intestinal conditional Ctr1 knockout (int) mouse. Main bands detected with Ctr2Ab are indicated with red arrows. Membrane was stripped and re-probed for actin, GAPDH and Ctr1. All molecular masses are indicated in kDa.

Ctr2 expression was analyzed in a mouse model for copper deficiency, the Ctr1 intestinal conditional knockout ($Ctr1^{int/int}$), in which only epithelial cells were lacking of Ctr1, while all the other peripheral tissues were homozygous for Ctr1 but copper deficient. Given the difficulty in generating such mice only two specimens were studied and were compared with control ($Ctr1^{flox/flox}$) mice of the same age.

All the bands detected by the mCtr2Ab showed higher expression levels in heart liver and brain of transgenic mice than in control animals (Fig. 11A, lanes 3-8, 13-14).

The 15kDa Ctr2 protein is significantly more expressed in kidneys of conditional Ctr1 knockout mice than control animals (Fig. 11A, lanes 9-10, and 11-12).

In contrast in the intestinal epithelial cells (IEC) of the $Ctr1^{int/int}$ mouse the 35kDa band seems to be downregulated when compared to the $Ctr1^{flox/flox}$, while the 15kDa band is basically not detectable in the Ctr1 null cells (Fig. 11A, lane 2; Fig. 11B, lane 2). Two different samples of intestinal epithelial cells collected from $Ctr1^{flox/flox}$ and $Ctr1^{int/int}$ were probed for Ctr2 expression, and a very similar result was obtained as shown in Fig 11B.

GAPDH and actin were used as loading controls and Ctr1 was used to confirm the identity and the genotype of the samples.

Ctr2 cellular localization

Initially different cell lines were screened as a model for immunolocalization experiments. Among these 3T3 was chosen because of its favorable morphological features, in particular the flat shape and the abundance of cytoplasm, which make them an excellent model for immunofluorescence experiments.
Cells were fixed with 3% paraformaldehyde and permeabilized with Triton-X 0.1%.
In comparison experiments, light intensity and contrast were adjusted to the same level.

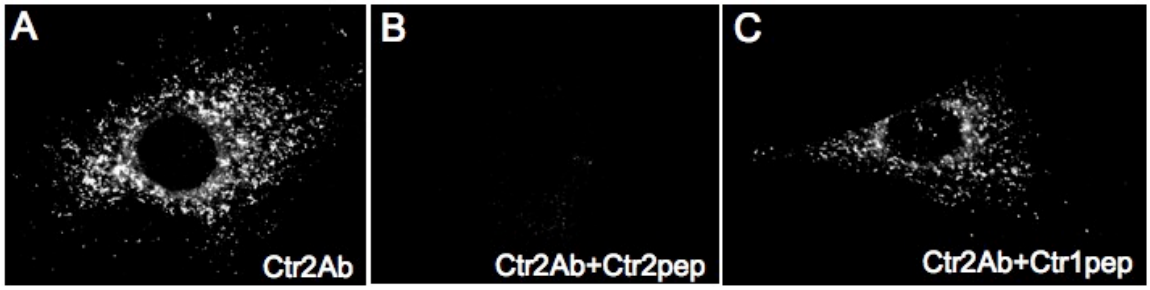

Figure 12. Indirect immunofluorescence analysis of an antibody competitionm assay. After the same fixation, permeabilization and blocking 3T3 cells were stained with different primary antibody solutions. A) Containing only Ctr2Ab. B) Containing Ctr2Ab and 80 molar excess of the homologous peptide. C) Containing Ctr2Ab and 80uM excess of a heterologous peptide. All cells were then labeled with AlexaFLuor 488 conjugated donkey anti-rabbit antibodies, and analyzed under the microscope.

An antibody-peptide competition assay was carried out to test specificity of the antibody, similar to what was previously done by immunoblot. As shown if Fig.12 pre-incubation of the mCtr2Ab with the peptide used as immunogen almost completely abolishes the staining (Fig. 12B). In contrast pre-incubation of the mCtr2 antibody with the same molar excess of a heterologous peptide, corresponding to Ctr1 C-tail sequence, doesn't affect the immunostaining (Fig. 12C).

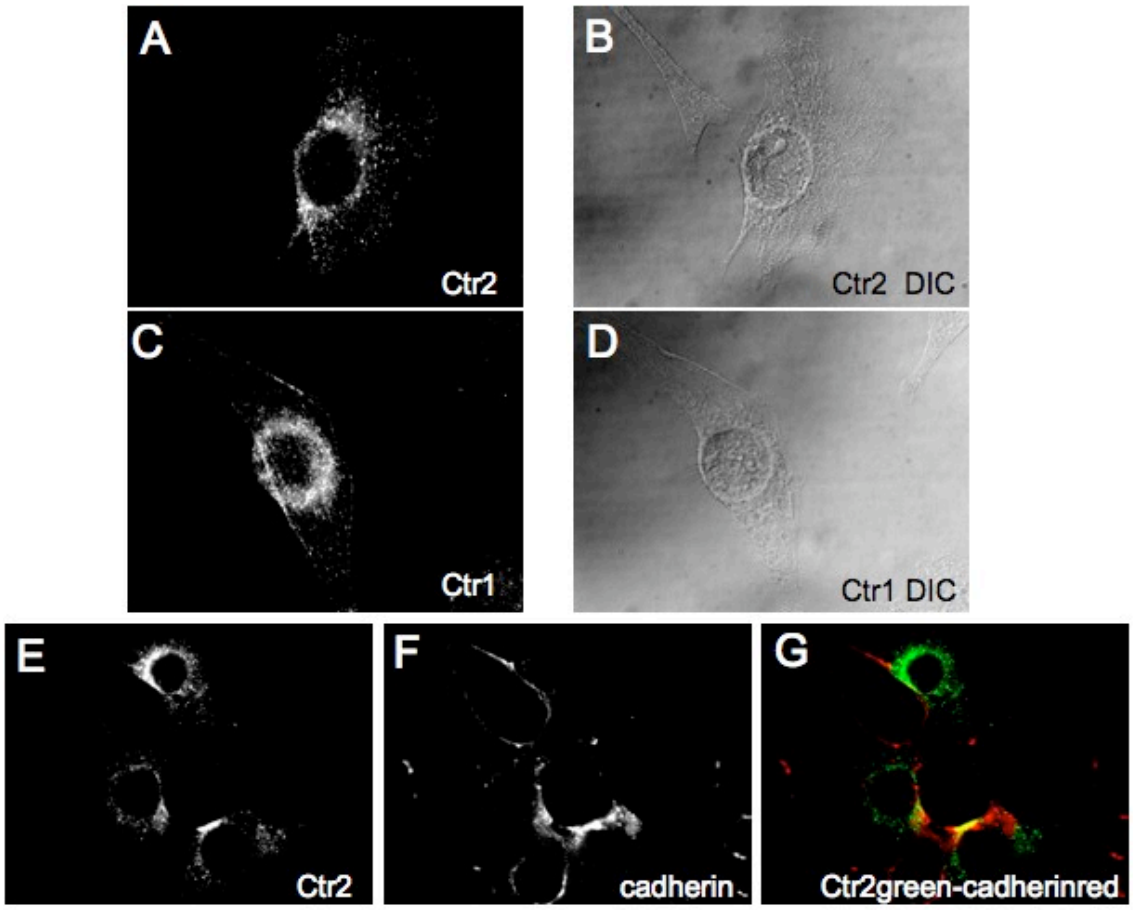

Figure 13. Analysis of 3T3 cells fixed with methanol at -20C and permeabilized with saponin. A and B) Cells labeled with Ctr2Ab followed by AlexaFLuor 488 conjugated donkey anti-rabbit antibodies. C and D) Cells labeled with Ctr1 antibody and with AlexaFLuor 488 conjugated donkey anti-rabbit antibodies. E-F) Cells were simultaneously labeled with Ctr2Ab followed by AlexaFLuor 488 conjugated donkey anti-rabbit antibody and CadherinAb followed by AlexaFLuor 568 conjugated goat anti-mouse antibody and G) Overlay.

During screening of different cell lines it was never observed plasma membrane staining with Ctr2 antibody. During such screening we tried to label cells with the Ctr1 antibody, but we failed to detect staining on the plasma membrane either. To rule out the possibility that the lack of plasma membrane signal was due to the fixation/permeabilization protocol it was used an alternative method applying ice-cold methanol for fixation and saponin 0.3% for permeabilization. Using such protocol we were able to detect plasma membrane staining with Ctr1 antibody (Fig.13B) but not with Ctr2 antibody (Fig. 13A). Figure 13G shows that while staining for Ctr2 is exclusively intracellular (green), staining for cadherin is mainly on the plasma membrane (red).
The yellow area in the figure is probably due to bleeding-through of the signal from the red channel into the green channel due to the strong intensity.

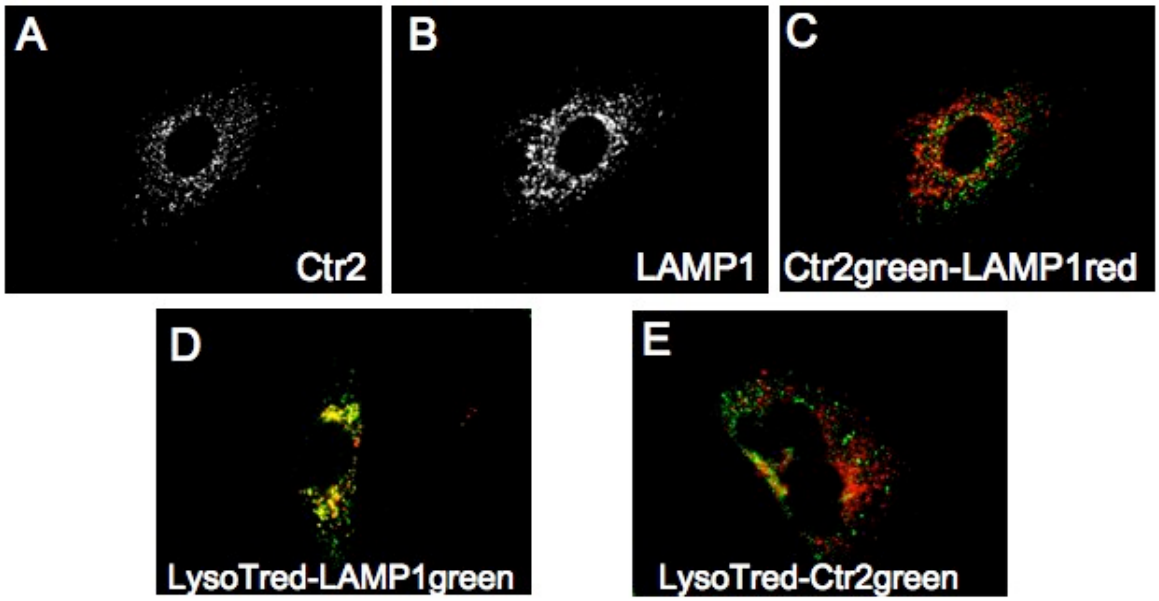

Figure 14. Analysis of 3T3 cells stained for Ctr2 and lysosomal markers. Cells were simultaneously labeled with Ctr2Ab (A), LAMP1 antibody (B) and (C) overlay. D) Overlay of green and red channels after staining with Lysotracker red and LAMP1Ab. E) Overlay of green and red channels after staining with Lysotracker red and Ctr2Ab.

Putative lysosomal localization was studied using two different markers: LAMP1 (lysosomal associated protein 1), one of the most abundant proteins found on the lysosomal membranes, and Lysotracker red (Invitrogen), a fluorescent dye that specifically labels vesicles/granules belonging to the lysosomal system. Ctr2Ab staining did not co-localize neither with LAMP1 (Fig 14C) nor with lysotracker (Fig. 14E) staining.
LAMP1 and lysotracker when used simultaneously resulted in a high degree of co-localization in large vesicles/granules, highlighted in yellow in Fig. 14D.

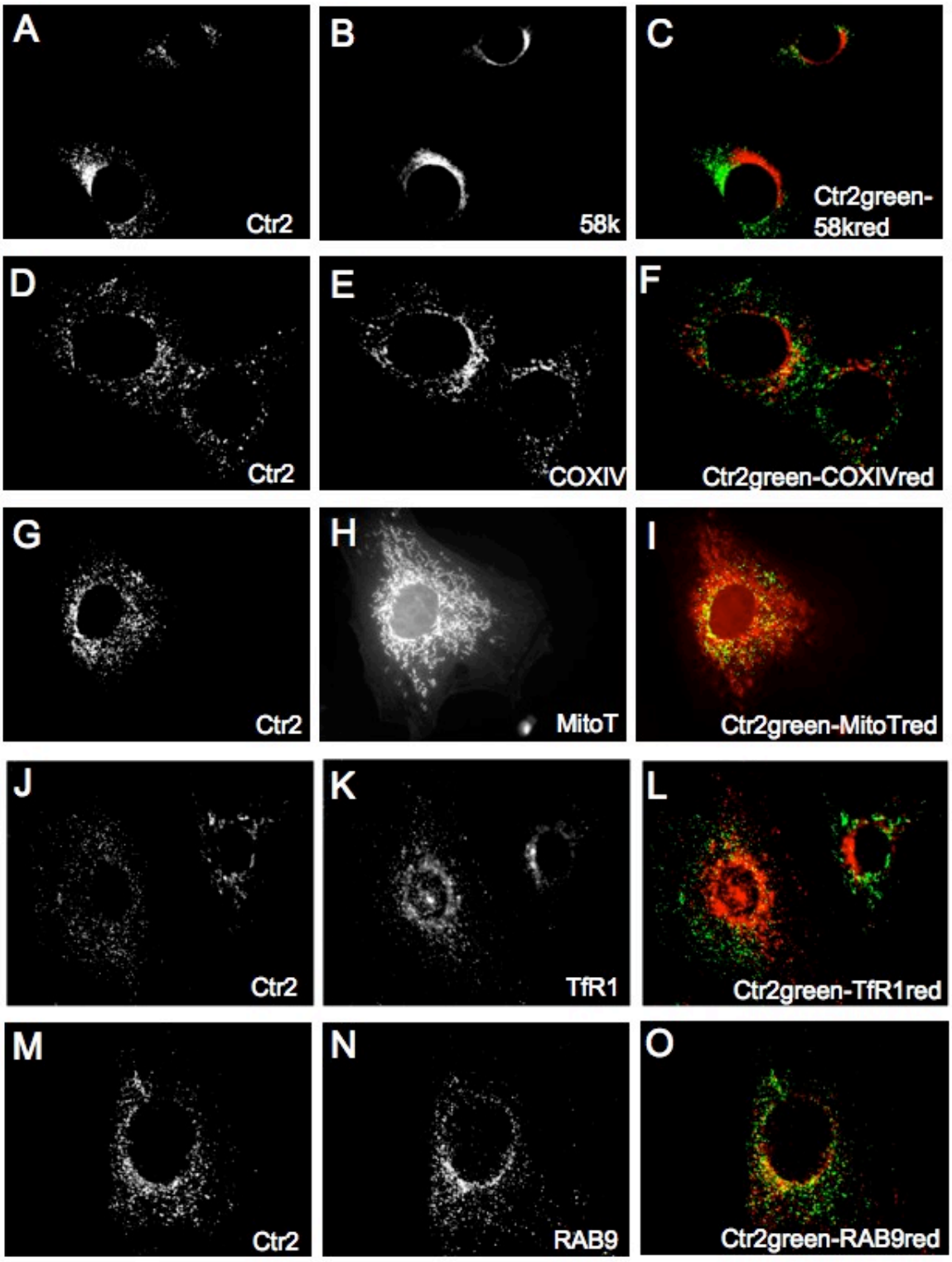

Figure 15. Analysis of 3T3 stained for Ctr2 and markers for the major subcellular compartments. A-B-C) 58kDa (Golgi). D-E-F) COXIV (Mitochondria) G-H-I) Mitotracker (Mitochondria) J-K-L) Transferrin Receptor 1 (recycling endosomes) M-N-O) RAB9 (late endosomes).

We also tested several markers for the major intracellular compartments: endoplasmatic reticulum PDI (data not shown), mitochondrial COXIV (Fig. 15E) and Mitotracker Red (Fig. 15H), 58kDa Golgi protein (Fig. 15B), mitochondrial COXIV (Fig. 15E), Mitotracker Red (Fig. 15H) and recycling endosomal TfR1 (Fig. 15K). Ctr2 staining (respectively FIG.15A-D-G-J-M) did not co-localize with any of these markers (Fig. 15C-F-I-L-O).
Only the RAB9 (Fig. 15N) staining partially co-localized with Ctr2 (Fig.15 M) as shown if Fig. 15O, yellow areas.
Finally we tested if copper supplementation or chelation in the growth media of E1 and E8 cells, could alter Ctr2 localization. Overnight copper starvation or excess did not alter Ctr2Ab staining pattern (data not shown). While the overall signal was very similar in both embryonic cell lines, in E8 cells we repeatedly observed a characteristic Ctr2 staining in granule-like structures (Fig. 16A), that strongly co-localized with LAMP1 (Fig. 16B), as shown in pictures 16C-D-E-F.

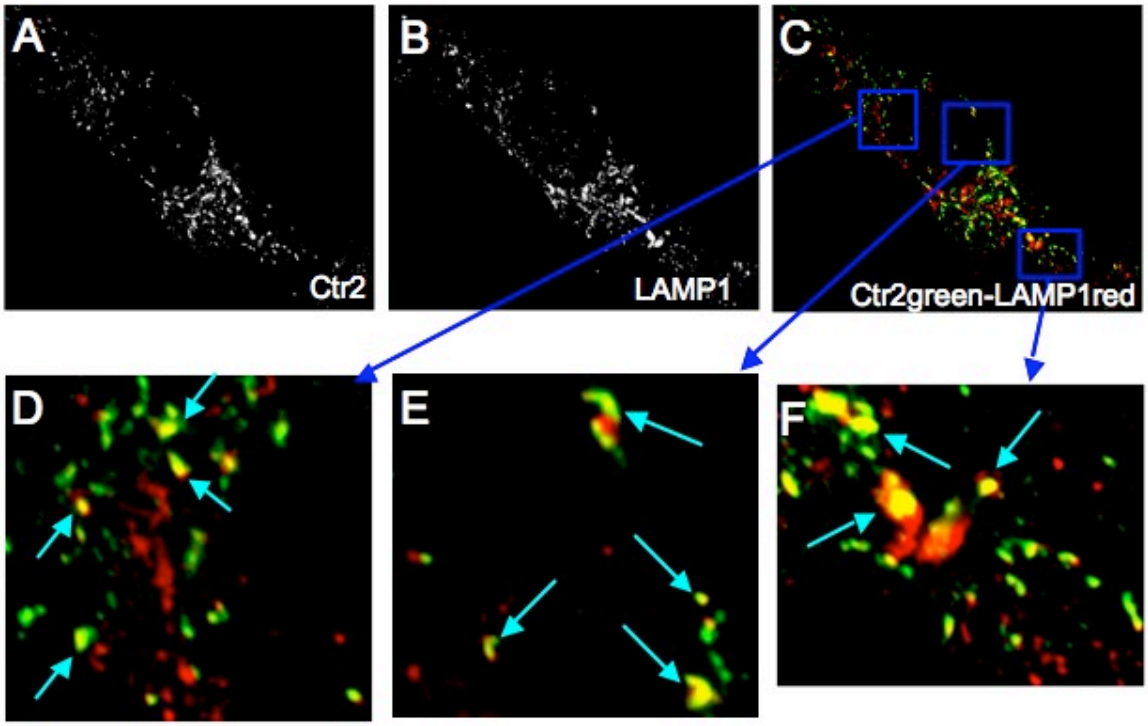

Figure 16. Analysis of E8 stained for Ctr2 and lysosomal marker LAMP1. Cells were simultaneously labeled with: A) Ctr2Ab followed by AlexaFLuor 488 conjugated donkey anti-rabbit antibody, B) LAMP1 antibody followed by AlexaFluor 568 conjugated goat anti-mouse antibody, C) Overlay of green and red channel, D-E-F) Higher magnifications of C, arrows in cyan highlight structures co-stained by both antibodies, in yellow.

4. Discussion and Conclusions

In the last decade many proteins involved in copper homeostasis have been identified, and particular interested has been focused on the high affinity copper transporters belonging to the Ctr family, whose members share sequence homology and likely structural and functional features (Dumay et al, 2006).
In mammals only two different members of this family have been identified, renamed Ctr1 and Ctr2 (Zhou and Gitschier, 1997). While the former has been extensively studied and many progresses have been made in understanding its cellular and physiological role, very little is known about the latter (Kim et al., 2008).
Very recently the structure of human Ctr1 has been resolved, confirming the hypothesis that this protein exists on the cellular membranes as homotrimer. Three identical subunits spanning the membrane layer three times, with intracellular C-term and extracellular N-term, assemble tail-to tail forming a pore-like channel at the center of the trimer (Allen and Unger, 2006; De Feo et al., 2009).
Generally in western blot experiments performed under denaturing conditions bands of different molecular weight have been detected using antibodies either to detect epitope-tagged chimeric (Lee et al., 2002a) or endogenous (Klomp at al., 2002) Ctr1 proteins. Such bands have been regarded by the experts in the field as monomeric and multimeric forms of Ctr1, despite their molecular weight is often variable and seems to be dependent on the biological sample and extraction conditions.
During this research with the anti Ctr1Ab developed in Dr. Thiele's laboratory, at Duke University, in cell lines and tissues we detected mainly and reproducibly a band of 17kDa apparent molecular weight. Recently a similar protein has been shown to be a cleaved version of the full Ctr1, produced in case of lacking of the O-glycosylation site at the Thr-27. Such proteolytic cleaved version of hCtr1 retains the ability to form dimers, is localized on the plasma membrane and promotes copper transport with halved rate compared to the full version (Marion et al., 2007). It is currently unknown if this proteolytic form differs from the full version in function, trafficking or signaling and plays a specific role in copper homeostasis.
Especially in cell lines, we often detected a smear around 35 kDa by immunoblitting with the hCtr1Ab. Detailed characterization studies carried out in human cell cultures revealed that the spaced smear of bands around 33-35 kDa mainly detected with different anti-Ctr1 antibodies, corresponds to the full length hCtr1 N-glycosylated at the Asp-15 and O-glycosylated at Thr-27 (Klomp et al., 2002; Eisses and Kaplan 2005b; Maryon et al., 2007).
Usually in tissues, the western blot pattern observed with different Ctr1 antibodies is more complex, and high molecular weight proteins, usually not found in cell lines, were detected (Kuo et al., 2006; Nose et al., 2006; Kim et al., 2008). Currently it is unknown if these multimeric forms represent physiological structures or are simply molecular artifacts due to aggregation during the extraction procedure.
No structural data are available yet for Ctr2, but given the partial structural homology with Ctr1 it is generally assumed that also Ctr2 may form multimers and possibly homotrimers.
Recently the Klomp group showed by co-immunoprecipitation experiments that human Ctr2 might interact with itself and possibly form multimeric complexes. However in such immunoprecipitation experiments from cells overexpressing Ctr2 constructs they observed only bands corresponding to the monomeric form (around 16 kDa) while bands of higher molecular weight were detected only upon chemical crosslinking (va den Berghe et al, 2007).
Bertinato et al. (2008) developed a human Ctr2Ab, which detected putative monomeric and dimeric forms when human Ctr2 was overexpressed as GFP-fused construct in cell lines. Only

a single protein of 70kDa was observed in cell lines and rat tissues only, argued to be a multimeric complex of endogenous human Ctr2 (Bertinato et al., 2008). Notably no endogenous monomeric form was detected. The difference in SDS-gel migration patterns due to epitope-tagging or over-expression is not currently understood, however Rees et al. reported that a yeast Ctr2 antibody detected by immunoblot mainly an endogenous Ctr2 protein corresponding to the monomeric form, while dimeric and trimeric complexes were observed when yeast Ctr2 was overexpressed by a plasmid (Rees and Thiele, 2007).
It is important to keep in mind that while mammalian Ctr1 and Ctr2 share high degree of sequence identity and similarity, mainly concentrated in the three transmembrane domains, their C-tail and N-term domain are quite different. Klomp group showed by yeast two-hybrid system how the N-terminal of Ctr1 interacts with itself, and how the methionine rich motif is important for such interaction. On the other hand the N-terminal of hCtr2 lacks this motif and indeed it does not interact with itself (Klomp et al., 2003). Recent works where hCtr1 oligomerization was studied by western blot experiments and structural analysis coupled to mutagenesis, suggested that detection of bands corresponding to Ctr1 dimeric forms are possibly related to inter molecular disulfide bridge formation, involving Cys-161 and Cys-189 in the C-terminal domain (Eisses and Kaplan, 2005b; Aller and Unger, 2006; Lee et al., 2007**;** De Feo et al., 2009). Ctr2 instead lacks these two cysteins.
Therefore structural and mutagenesis studies will be necessary to reveal the putative holigomerization mechanism allowing Ctr2 multimerization and which aminoacids are important in this process.
The mCtr2Ab developed in Dr. Thiele's laboratory was able to detect 3 main endogenous proteins in western blot experiments, respectively around 15, 35 and 70kDa.
Three different lines of evidence support the hypothesis that the 15 kDa represents the monomeric form of mouse Ctr2:

1) Its molecular weight matches the one expected from the coding sequence of the mCtr2 gene.
2) Overexpression of hCtr2 tagged constructs in different human cell lines resulted in the detection of a similar band in western blotting. The main and most notable difference is that we were able to detect the endogenous protein not only in all cell lines but also in mouse tissues, although to accomplish this goal a modification of the protein extraction protocol was required.
3) RNAi oligonucleotides targeting the mouse Ctr2 mRNA caused a marked and time dependent decrease of its expression

The 35kDa, based on the apparent molecular weight may represent a dimeric form, and could correspond to one of the multimers detected upon chemical crosslinking by van der Berghe et al. The 70kDa band could be the same multimeric form detected by Bertinato et al. in rat tissues. The expression of these proteins did not alter following RNAi knockdown of the Ctr2 gene. It is not possible to rule out the possibility that such bands may represent multimeric and very stable molecular complexes with a very long hemi-life. This might be in accordance with the fact that Bertinato et al. (2008) were able to obtain a partial silencing of the 70kDa band only after 96 hours and a double RNAi transfection using siRNA duplexes targeting human Ctr2 mRNA. This hypothesis hardly explains how after a very robust silencing of the monomeric form from 48 almost until 120h, the expression of the putative multimeric form is not affected at all either. Interestingly the three bands show also different and peculiar biochemical properties.
Interestingly the three bands show different and unusual biochemical properties. While the 15 and the 35kDa bands are associated with a pelletable fraction the 70kDa band is mainly, but not exclusively, associated with the soluble fraction after homogenization in a free detergent buffer and centrifugation at 100,000g.

Furthermore the 15kDa and the 35kDa bands show different enrichment patterns in fraction obtained after differential centrifugation, and while the former is sensitive to heat treatment, like most of the membrane associated proteins, the latter is not. It is known that boiling has a counterproductive effect on the detection of membrane proteins indeed Ctr1 and Lamp1 show heat sensitivity like the 15kDa protein. Instead, the 35kDa protein, despite its association with the pelletable fraction that suggests association with biological membranes, seems to be an exception to this rule.
Failure in detecting the 15kDa band by immunoblot probably explains why Bertinato et al., were not able to detect hCtr2 momoner, since they boiled samples prior to loading onto SDS-PAGE (Bertinato et al., 2008).
According to our immunoblot experiments both 15 and 35kDa bands were more abundant in testis, liver, kidney, and less expressed in heart and brain in accordance to the transcription levels previously reported in the mouse (Lee et al., 2000) and the hCtr2 protein levels with the exception of the heart, where hCtr2 was reported to be highly expressed (Bertinato et al., 2008). As for Ctr1, in all tissues analyzed and in particular liver and kidney several new bands, not observed in cell lines, were detected. Interestingly liver and kidney are also the tissues where Ctr1 is highly expressed, even if it's known that Ctr1 levels vary according to age and copper availability (Kuo et al., 2006).
The 15kDa and 35kDa bands not only show different biochemical properties but also a different expression in relation to copper and Ctr1 levels. It is still debated how Ctr1 is regulated following copper exposure. Some works reported how elevated extracellular copper levels resulted in a rapid internalization from plasma membrane and subsequent degradation of hCtr1, with a mechanism involving the C-terminal Methionine-rich domain (Petris et al., 2003; Guo et al., 2004), similarly to what reported for yeast Ctr1 (Ooi et al., 1996; Liu et al., 2007).
Other authors reported no changes in Ctr1 levels or localization following copper exposure (Klomp et al., 2002; Eisses et al., 2005a). It is likely that such differences might reflect cell or tissue specific regulation.
Addition of copper to growth media slowly reduced in time dependent manner the expressions of 15kDa proteins in RAG cells. The decrease in Ctr2 levels started after 24h of copper exposure and became significant only after 48h. Notably the time and copper dependent Ctr2 downregulation takes place in parallel with a decrease in CCS levels. CCS is a cytosolic copper chaperone that delivers copper ions to CuZn SOD1 (Culotta et al., 1997) and has been shown to be regulated by a copper induced degradation, and for this reason it was proposed as a biomarker for cytosolic copper bioavailability (Bertinato and L'Abbe, 2003). Based on this result it is possible to hypothesize that prolonged exposure to copper leads not only to a degradation of CCS but also of Ctr2.
If mammalian Ctr2, as its yeast hortologue, transports copper from an intracellular compartment to the cytosol, it would make sense for the cells to coordinate downregulation of Ctr1 and Ctr2 in case of high levels of copper in the extracelluar environment. This regulation would be necessary in order to prevent accumulation of high and toxic metal concentrations in the cytosol.
We did not observe any re-localization of endogenous Ctr2 following 24h copper exposure (data not shown) as previously reported for an overexpressed tagged version (van den Berghe et al., 2007), but this might be due to the short exposure time.
The most interesting and unexpected difference that further marks the difference between the 15kDa and 35kDa protein expression, is what appears to be a Ctr1 dependent regulation.
Two distinct mice Ctr1 knock out cell lines, derived from embryos of Ctr1 knock out mice have been described. Those cell lines are viable despite lack of Ctr1 and have been shown to possess a low affinity Ctr1-independent copper import system (Lee et al., 2002b). We expected that in cells the chronicle copper starvation could induce expression of Ctr2 as

compensatory mechanism. Surprisingly we found that in those cells the expression level of the 15kDa band is strongly and permanently downregulated, but not completely abrogated. On the other hand the 35 and 70kDa proteins levels are not affected by the absence of Ctr1.
To assess if the Ctr1 dependent downregulation was induced by copper starvation we studied Ctr2 expression in copper starved and repleted E1 (WT) and E8 ($Ctr1^{-/-}$) cell lines. Twenty four hours of exposure to copper chelator BCS induced in both cell lines an increase in 35kDa band, as well as a significative increase in 15kDa expression in wild type cell lines. Instead in Ctr1 null cell lines the 15kDa protein downregulation is not reversible neither following copper starvation.
To assess if this downregulation was due to the physical lacking of Ctr1 or to the chronicle copper starvation that affects Ctr1 null cells we investigated Ctr2 expression in Villin-CRE intestinal conditional Ctr1 knock out mice. These mice were generated in Dr. Thiele's laboratory by breeding Ctr1 flox mice with mice expressing the CRE recombinase under the control of a villin-promoter, which is actively expressed only in intestinal epithelial cells. As result the Villin-CRE intestinal conditional Ctr1 express Ctr1 in all tissues but intestinal epithelial cells (IEC). Biochemical characterization of those animals highlighted the role of Ctr1 in diet copper absorption, since deletion of Ctr1 in IEC cells causes peripheral copper depletion in basically all tissues and severe growth impairment.
We reasoned that given the simultaneous presence of cells lacking of Ctr1 and copper deficient cells in the same organism, these mice could be the perfect model to study *in vivo* the Ctr1-dependent Ctr2 regulation. Despite more samples need to be examined our preliminary results seem to confirm the hypothesis that the physical lack of Ctr1 induces monomeric Ctr2 downregulation, while in copper starved tissues its expression is unaltered, or, like in kidney, upregulated. Since kidney was shown to be the tissue were copper deficiency was less severe in these mice, it is tempting to speculate that upregulation of Ctr2 and possibly Ctr1 may counteract low copper concentrations in the blood.
van den Berghe et al. (2007) speculated that hCtr2 mediates copper uptake in Ctr1 null cell lines and IEC, mobilizing lysosomal copper stores uptaken by endocytosis. Based on their data hCtr1 works as a high affinity transporter, while hCtr2 copper uptake works with low affinity and requires either high concentration of extracellular copper or prolonged exposure in order to provide significant copper levels to the cytosol. According to their model the Ctr2 low affinity copper uptake would explain why the Ctr1 conditional intestinal knockout mice still suffer of sever copper deficiency (van den Berghe et al., 2007). Bertinato et al. (2008) proposed a similar model where Ctr2 functions as low affinity plasma membrane transporter alternative to Ctr1. They also speculate according to this model that Ctr2 may compensate loss of Ctr1 in tissues of heterozygous mice, or could replace Ctr1 mediated copper import when extracellular copper levels are elevated enough to induce Ctr1 internalization (Bertinato et al., 2008). Our experiments indicating that Ctr2 monomer expression is actually almost completely abrogated in Ctr1 null cells and partially downregulated in liver of Ctr1 heterozygous mice, and prolonged exposure decrease its expression as well, would suggest that these hypothesis are unlikely.
The identity of the 35 kDa protein remains enigmatic.
Despite the RNAi results, the biochemical features and the apparent lack of copper/Ctr1 dependent regulation two lines of evidence suggest that the possibility of the 35kDa band recognized by the mCtr2Ab being a non-Ctr2 related specific protein is unlikely. First, despite the fact that the peptide used as immunogen has a unique sequence in the mouse proteome and the antibody was isolated by affinity purification the antibody seems to bind the 35kDa protein with an affinity similar or superior to the one for Ctr2 monomeric protein. Second, its relative expression levels in different cell lines and tissues match the expression levels of Ctr2 monomeric form.

From the results here reported three main hypotheses about the nature of 35kDa protein can be formulated:

1) This protein could be the product of an alternative Ctr2 transcript, not harboring the nucleotidic sequence targeted by the RNAi oligos used in knockdown experiments and differently regulated by either copper or Ctr1. Interestingly in yeast at least three different Ctr2 transcripts carrying different 3' UTR regions were identified, and one of them seems to confer a copper resistant phenotype (Kim Guisbert et al., 2007). In the mouse database genome at least three different Ctr2 transcripts are annotated but the fact that all of them contain the same coding sequence would not explain the different migration and biochemical properties of 15kDa and 35kDa proteins. Notably northern blot analysis in rat tissues revealed the existence of two discrete Ctr1 transcripts (Lee et al., 2000).
2) The mouse genome may code for a Ctr2 pseudogene, not yet annotated in the databases. Interestingly Møller and colleagues identified a hCtr1 pseudogene mapping on a different chromosome, transcriptionally active, but not inducing a copper phenotype when transfected in human cells (Møller et al., 2000). This hypothesis, although unlikely, could explain the different biochemical properties and regulation.
3) It is possible that under conditions used for protein isolation Ctr2 may form SDS-resistant and heat resistant aggregates as reported for other membrane proteins (Kubista et al., 2004). SDS resistant multimeric complex caused by oxidation of cysteins residues and inter molecular disulfide bridge formation have been described also for soluble proteins the most notable of which is metallothionein (Haase and Maret, 2008). Ctr2 lacks cysteine residues and protein aggregation could be caused by to oxidation of methionine residues. In alternative the highly hydrophobic nature of its aminoacidic sequence may not allow a complete denaturation mediated by SDS, resulting in a non linear migration patterns and appearance of high molecular weight bands. In either case apparently constant levels under conditions where the Ctr2 monomer expression is radically altered could be explained by the high affinity of these putative complexes for the PDVF membrane used in western blotting. In this case even very low amount of complexes in the protein extracts could easily bind to the membranes leading to a strong signal. This hypothesis could explain both the different biochemical properties and the apparent different regulation of the 15kDa and 35kDa proteins.

Given the contradictive results for the two main proteins detected by the mCtr2Ab only analysis of tissues and cells from Ctr2 knock out mice or in alternative mass fingerprinting, will allow to determine if this protein is a multimeric form of mouse Ctr2 or the product of a different gene.

Another goal of this research was to identify the cellular localization of endogenous mouse Ctr2. While the yeast hortologue has been localized to the vacuolar membrane mammalian Ctr2 localization is still controversial. To accomplish this goal we tested different mouse cell lines by indirect immunofluorescence experiments. In all cell lines we always detected a perinuclear punctate signal, which we were not able to clearly co-localize with any of the markers for the main subcellar compartments.

van den Berghe et al. (2007) showed that in several cell lines the overexpression of different hCtr2 tagged constructs localized in same large vesicles. Such vesicles also contained lysosomal markers LAMP1 and LAMP2. Given this result and the biological analogies between yeast vacuole and mammalian lysosomes they proposed that hCtr2 localizes in the lysosomal membranes. In order to verify this hypothesis we tested mCtr2Ab with two different markers, Lysotracker (Molecular Probes) a lysosomal specific dye, and LAMP1, one of the most abundant proteins in the lysosomes. Both markers stained mainly large vesicles/granules typical of the mature lysosomal compartment, similar to the ones reported by van den Berghe and colleagues. Furthermore when used simultaneously they had a high

degree of co-localization in such structures. The morphology of the typical intracellular staining typical mCtr2Ab was different from the one described above, and indeed neither Lysotracker nor LAMP1 staining co-localized with the Ctr2 signal. Bertinato and colleagues studied in parallel localization of endogenous and epitope tagged overexpressed hCtr2. Interestingly while a GFP-tagged construct strongly localized in large cytoplasmic vesicles, similarly to what previously reported by the other group, the staining pattern detected by the antibody was completely different, punctuate and perinuclear, similar to what we observed. Unfortunately they did not further investigate the identity of such compartment (Bertinato et al., 2008).

The simultaneous overexpression of hCtr1 and hCtr2 constructs harboring different epitope-tags in human cells resulted in a partial co-localization of the two Ctr members in intracellular vesicles (van den Berghe et al., 2007). Given the strong co-localization of the hCtr2 construct with lysosomal markers, this experiment would suggest at least a partial localization of hCtr1 in lysosomes, but this result is in contrast with the literature.

In fact previous studies revealed that endogenous Ctr1 can recycle and traffic between the plasma membrane and small intracellular vesicles, and its main steady-state localization was probably dependent on the cell line studied (Klomp et al 2002; Lee et al., 2002a; Eissen and Kaplan, 2005a). While the identity of this intracellular compartment remains elusive a previous studies from the same group suggested the small vesicles partially co-localizing with TGN (Trans Golgi Network) markers but not with lysosomal markers (Klomp et al, 2002; Komp et al., 2003). Notably also the ATPase copper transporter ATP7a and ATP7b normally reside on the TGN and can traffic and re-localize to the plasma membrane after copper exposure (La Fontaine and Mercer, 2007).

Other groups reported a partial localization of Ctr1 in recycling endosomes containing Transferrin Receptor 1 (Petris et al., 2003; Kelleher and Lönnerdal 2006).

In our experiments we did not observe co-staining of mCtr2Ab neither with TfR1 nor 58kDa, a Golgi marker, but we found a partial co-localization with RAB9, a GTPase involved in vesicle retrograde transport from the endosomal compartment to the Trans Golgi Network (Lombardi et al., 1993; Bonifacino and Rojas, 2006).

If this localization will be confirmed it would be possible to hypothesize that endogenous Ctr2 resides at steady state levels in a part of the Trans-Golgi network, possibly at the interface with the endosomal compartment, highlighting the possibility that all four major mammalian membrane copper transporters might traffic to the same compartment. A copper fluorescent dye, named copper sensor 1 (CS1), allowing detection of free copper pools in living cells was developed by Zeng et al. (2006). Interestingly such copper pools seem to be contained in vesicle-like structures that partially co-localize with fluorescent dyes specific for the Trans Golgi Network (Dr Chang CJ, personal communication). Together these observations would suggest the intriguing possibility of the existence of copper specialized vesicles in a subcellular compartment belonging to the Trans Golgi Network. Without stronger evidences such hypothesis remains just a speculation.

It was not possible for us to test via indirect immuofluorescence the intriguing hypothesis of a partial co-localization between endogenous Ctr1 and Ctr2, only indirectly suggested by differential centrifugation experiments, because both antibodies were raised in the rabbit.

Bertinato and colleagues detected a low intensity staining on the plasma membrane using the hCtr2 antibody, suggesting a partial localization on the cell surface, despite the epitope-tagged form does not seem to stain the plasma membrane (Bertinato et al., 2008) as previously reported by the Klomp group (van den Berghe et al., 2007). The cell surface result was confirmed by biotinilation experiments carried out in human, for both overexpressed and endogenous proteins. During our fluorescence studies carried out in several mouse cell lines, we have never observed a plasma membrane staining related to endogenous hCtr2. To rule out the possibility that lack of plasma membrane detection was due to incorrect fixation-

permeabilization of the cells we employed two different protocols. Interestingly while detection of endogenous hCtr1 on the plasma membrane was abrogated using paraformaldehyde and Triton-X, it was clearly visible using methanol and saponin. Instead the mCtr2Ab signal was not affected by the protocol and in both cases the staining was exclusively intracellular and perinuclear.

Despite the results presented by Bertinato and colleagues seem controversial, further studies will be required to verify the possibility of mammalian Ctr2 to localize or traffic to the plasma membrane. One hypothesis that could explain the staining on the plasma membrane only in human cells but not in mouse cells could be the presence in the human genome of a alternative Ctr2 variant not found in the mouse genome. Such variant differs from the more common and conserved mammalian Ctr2 for the additional presence of 60 aminoacids in the N-terminal of the protein (Zhou and Gitschier, 1997). The N-terminal sequence could harbor signals driving the protein to the plasma membrane. Further studies will be required to characterize this form and its putative role in copper metabolism.

Alternatively the two distinct staining patterns reported by the L'Abbe group could suggest that endogenous and over-expressed hCtr2 may localize in two different compartments (Bertinato et al., 2008). It is known that overexpression of proteins in cells can alter their proper localization (Miyashita, 2004). This hypothesis is supported by our results too, even if we cannot rule out the possibility that the antibody developed in Dr. Thiele's laboratory may recognize a specific protein other than Ctr2 not only by immunoblot but also by indirect immunofluorescence.

Two more indirect observations support the hypothesis that Ctr2 does not localize in lysosomal membranes, and this mis-localization might be due to overexpression of the epitope tagged Ctr2. A general signature of lysosome membrane proteins is a high degree of glycosilation aimed to protect them from the proteolytic enzymes in the lysosomal lumen (Eskelinen et al., 2003) but immunoblot and lacking of glycosylation consensus sequences would suggest that Ctr2 is not glycosylated. Furthermore two independent mass spectrometry based proteomics studies aimed to map the lysosome proteome did not identify Ctr2 among the lysosomal resident membrane proteins (Bagshaw et al., 2005; Schröder et al., 2007).

Interestingly in the Ctr1 null cell lines, where by immunoblot we observed a constitutive downregulation of the 15kDa protein, we detected a unique Ctr2 immunostaining pattern. Surprisingly while the overall staining intensity was not different from the one detected in wild type mouse embryonic cell lines, we noticed a characteristic staining of intracellular granules similar. Such structures reminded us the same structures co-localizing with overexpressed human Ctr2, indeed they were positive for LAMP1 staining, proving they belonged to the lysosomal system.

This result led us to perform an analysis of conserved motifs in the primary sequence of mammalian Ctr2 proteins, which revealed the presence of at least two different putative lysosomal targeting sequences highly conserved in all species analyzed. A D[E]XXXL[LI] in the N-terminus of the protein, preceded by a conserved serine, could suggest the possibility that upon phosphorylation mediated activation, this signal may mediate Ctr2 lysosomal targeted degradation, as it was demonstrated for tow cell surface receptors, CD3 (Dietrich et al., 1994; Pitcher C et al., 1999) and CD4 (Pitcher C et al., 1999). Three putative YXXØ signals, two of which are preceded by a glycine may also be involved in lysosomal targeting. It is not clear if these tyrosine motives are accessible to the sorting machinery or not, given their proximity to the putative transmembrane domains. Furthermore is currently unknown that two distinct targeting signals in the same protein affect trafficking to the lysosomes (Braulke and Bonifacino, 2008). Interestingly these three motives are also present in the animal Ctr1 sequence. Given the evidences that binding of copper to the MXXXM motif may induce conformational change (De Feo et al., 2009), and the same motif is essential for copper dependent Ctr1 internalization and degradation (Guo et al., 2004) it is possible the two

tyrosine based signals flanking the MXXXM motif, might become exposed after copper binding and therefore mediating the copper dependent internalization and degradation of both Ctr1 and Ctr2.
Notably it has been shown that over-expression of proteins bearing either type of signal leads to saturation of the sorting machinery, affecting either localization or recycling of other proteins containing the same signals (Marks et al., 1996). In case that the tyrosine based signals shared by Ctr1 and Ctr2 are responsible for copper induced Ctr1 internalization, it is possible that the increased copper uptake activity induced by hCtr2 overexpression previously reported (van den Berghe et al., 2007; Bertinato et al., 2008), may be due to inhibition of downregulation of human and not directly correlated to Ctr2 activity.
An other important goal of the research was to study the phenotype induced by RNAi mediated knockdown of Ctr2 in mouse cells, in order to shed light about its function and putative role in copper homeostasis.
When we tested Ctr1 levels in Ctr2 silenced cells, we discovered that also the expression of the Ctr1 fragment was significantly reduced compared to control cells, while the full and glycosylated form seemed unaffected. This intriguing observation had a major drawback in determining Ctr2 activity, because downregulation of Ctr1 and consequent copper uptake reduction would mask Ctr2 activity.
Lack of data excluding that Ctr1 downregulation is not due to off-target effects of Ctr2 targeting RNAi oligos, it's only speculative to hypothesize that Ctr1 expression is directly affected by Ctr2 expression levels, possibly by a post-transcriptional regulation mechanism. However if confirmed, this result would suggest that Ctr1 and Ctr2 are not only regulated in a coordinate way, but also able to reciprocally modulate each other's expression.
Based on the results present in this research and the bibliographic reports, it can be proposed a model where mammal Ctr2 is mainly localized in small cytoplasmic vesicles containing copper pools and possibly belonging to the Trans Golgi Network. In this model Ctr2 expression is coordinated with Ctr1 expression in a copper dependent and in a copper independent way. In the copper dependent way an excess of copper induces downregulation of both membrane transporters while copper starvation induces upregulation of their expression. In the copper independent way Ctr1 expression is required for Ctr2 expression and localization and lack of Ctr1 induces Ctr2 degradation possibly through trafficking of Ctr2 in the lysosomes mediated by lysosomal targeting signals.
This regulation may suggest that the cells interpret the absence of Ctr1 as signal for excess of copper in the extracellular environment, and this signal triggers Ctr2 degradation as defensive mechanism to avoid copper overload.
A possible mechanism allowing the coordinate regulation of Ctr1 and Ctr2 expression in response to copper levels is shown in Fig. 1
In higher eukaryotes a Ctr1-Ctr2 intermolecular interaction in intracellular compartment where Ctr2 localizes at steady state levels would mask the lysosomal sorting signals harbored in both proteins, preventing them to be bound and recognized by the sorting machinery.
This interaction could be either inhibited directly by high concentrations of copper, or by a third protein "sensing" copper overload.
In either case this copper dependent interaction could be the checkpoint influencing the destiny of Ctr1 after internalization from the plasma membrane as well the destiny of Ctr2: low copper levels would allow the interaction and the partial recycling of Ctr1 to the plasma membrane, not affecting Ctr2 steady state levels (Fig. 1 upper panel). Instead high cytosolic copper concentrations would cause inhibition of the Ctr1-Ctr2 interaction re-directing both proteins to the lysosomes for protein degradation (Fig.1 lower pane).
Lack of either protein would cause a disruption of the "homeostatic balance" leading to a massive and constitutive trafficking of the counterpart to the lysosomes for protein degradation. This scenario could explain why in Ctr1 null cells Ctr2 protein levels are

extremely low, and why Ctr2 RNAi mediate knockdown causes a similar decrease in Ctr1 protein levels, in particular of the proteolytic cleaved form of Ctr1.
A physical interaction and a copper dependent co-regulation of two distinct members of the Ctr family has been described in the yeast *S. pombe* (Zhou and Thiele, 2001).
This model does not exclude but actually favors the possibility suggested by bibliographic and structural data that Ctr2 might function as an intracellular low affinity copper transporter. The Ctr1-Ctr2 interdependent regulation would allow the cells to coordinate copper influx from the extracellular environment and from the intracellular stores.
More studies will be required to confirm this hypothesis and to determine the functions and the role in copper homeostasis of this elusive protein.

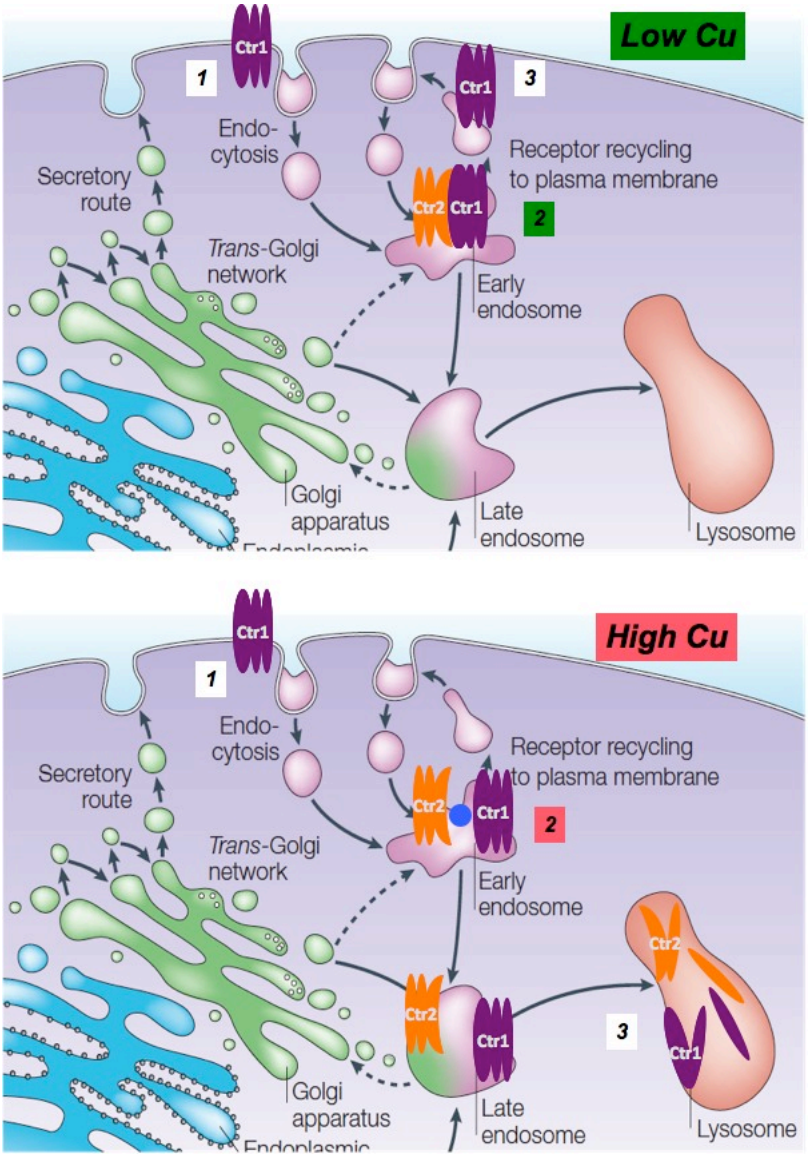

Figure 1. Proposed model for Ctr1/Ctr2 regulation in which interaction between the two Ctr members function as a checkpoint. At low copper concentrations (upper figure) when Ctr1 is internalized can interact with Ctr2 in an intracellular compartment. This interaction stabilizes both proteins and Ctr1 can be recycled to the plasma membrane. At high copper concentrations (lower figure) when Ctr1 is internalized the interaction is inhibited either by copper or a copper sensing protein binding protein inhibit their interaction cannot interact Both proteins are targeted to the lysosomes where they are degraded.

Acknowledgments

I would like to thank my parents for letting me choose my education and for supporting me in many ways during all these years.
I would like to thank Prof. Emilio Carpenè for being my advisor in this PhD and giving me the opportunity to do research abroad.
I would like to thank Dr. Dennis J. Thiele for having me as research scholar in his lab at Duke University and assigning me the mCtr2 project, and all the Thiele laboratory members for useful and stimulating scientific discussions.
Last but not least a very special thanks to Her, for assisting me in revising this thesis and especially for supporting me during the tough times.

5 References

1) Aller SG, Eng ET, De Feo CJ, Unger VM. Eukaryotic CTR copper uptake transporters require two faces of the third transmembrane domain for helix packing, oligomerization, and function. *J Biol Chem*, 2004;279(51):53435-41.

2) Aller SG, Unger VM. Projection structure of the human copper transporter CTR1 at 6-A resolution reveals a compact trimer with a novel channel-like architecture. *Proc Natl Acad Sci U S A*, 2006;103(10):3627-32.

3) Andreini C, Banci L, Bertini I, Rosato A. Occurrence of copper proteins through the three domains of life: a bioinformatic approach. *J Proteome Res*, 2008;7(1):209-16.

4) Argüello JM, Eren E, González-Guerrero M. The structure and function of heavy metal transport P1B-ATPases. *Biometals*, 2007;20(3-4):233-48.

5) Bagshaw RD, Mahuran DJ, Callahan JW. A proteomic analysis of lysosomal integral membrane proteins reveals the diverse composition of the organelle. *Mol Cell Proteomics*, 2005;4(2):133-43.

6) Banci L, Bertini I, Cantini F, Felli IC, Gonnelli L, Hadjiliadis N, Pierattelli R, Rosato A, Voulgaris P. The Atx1-Ccc2 complex is a metal-mediated protein-protein interaction. *Nat Chem Biol*, 2006;2(7):367-8.

7) Banci L, Bertini I, Cantini F, Massagni C, Migliardi M, Rosato A. An NMR study of the interaction of the N-terminal cytoplasmic tail of the Wilson disease protein with copper(I)-Hah1. *J Biol Chem*, 2009 [Epub ahead of print].

8) Bauerly KA, Kelleher SL, Lönnerdal B. Functional and molecular responses of suckling rat pups and human intestinal Caco-2 cells to copper treatment. *J Nutr Biochem*, 2004;15(3):155-62.

9) Bellemare DR, Shaner L, Morano KA, Beaudoin J, Langlois R, Labbe S. Ctr6, a vacuolar membrane copper transporter in *Schizosaccharomyces pombe*. *J Biol Chem*, 2002;277(48):46676-86.

10) Bertinato J, L'Abbé MR. Copper modulates the degradation of copper chaperone for Cu,Zn superoxide dismutase by the 26 S proteosome. *J Biol Chem*, 2003;278(37):35071-8.

11) Bertinato J, Swist E, Plouffe LJ, Brooks SP, L'abbé MR. Ctr2 is partially localized to the plasma membrane and stimulates copper uptake in COS-7 cells. *Biochem J*, 2008;409(3):731-40.

12) Bonifacino JS, Rojas R. Retrograde transport from endosomes to the trans-Golgi network. *Nat Rev Mol Cell Biol*, 2006;7(8):568-79.

13) Bonifacino JS, Traub LM. Signals for sorting of transmembrane proteins to endosomes and lysosomes. *Annu Rev Biochem*, 2003;72:395-447.

14) Braulke T, Bonifacino JS. Sorting of lysosomal proteins. *Biochim Biophys Acta*, 2008 [Epub ahead of print].

15) Brown NM, Torres AS, Doan PE, O'Halloran TV. Oxygen and the copper chaperone CCS regulate posttranslational activation of Cu,Zn superoxide dismutase. *Proc Natl Acad Sci U S A*, 2004;101(15):5518-23.

16) Carpenè E, Andreani G, Isani G. Metallothionein functions and structural characteristics. *J Trace Elem Med Biol*, 2007;21 S1:35-9.

17) Caruano-Yzermans AL, Bartnikas TB, Gitlin JD. Mechanisms of the copper-dependent turnover of the copper chaperone for superoxide dismutase. *J Biol Chem*, 2006;281(19):13581-7.

18) Chen H, Su T, Attieh ZK, Fox TC, McKie AT, Anderson GJ, Vulpe CD. Systemic regulation of Hephaestin and Ireg1 revealed in studies of genetic and nutritional iron deficiency. *Blood*, 2003;102(5):1893-9

19) Cobine PA, Ojeda LD, Rigby KM, Winge DR. Yeast contain a non-proteinaceous pool of copper in the mitochondrial matrix. *J Biol Chem*, 2004;279(14):14447-55.

20) Cobine PA, Pierrel F, Bestwick ML, Winge DR. Mitochondrial matrix copper complex used in metallation of cytochrome oxidase and superoxide dismutase. *J Biol Chem*, 2006;281(48):36552-9.

21) Culotta VC, Klomp LW, Strain J, Casareno RL, Krems B, Gitlin JD. The copper chaperone for superoxide dismutase. *J Biol Chem*, 1997;272(38):23469-72.

22) Dancis A, Haile D, Yuan DS, Klausner RD. The *Saccharomyces cerevisiae* copper transport protein (Ctr1p). Biochemical characterization, regulation by copper, and physiologic role in copper uptake. *J Biol Chem*, 1994;269(41):25660-7.

23) Davis AV, O'Halloran TV. A place for thioether chemistry in cellular copper ion recognition and trafficking. *Nat Chem Biol*, 2008;4(3):148-51.

24) De Feo CJ, Aller SG, Siluvai GS, Blackburn NJ, Unger VM. Three-dimensional structure of the human copper transporter hCTR1. *Proc Natl Acad Sci U S A*, 2009. [Epub ahead of print]

25) Dietrich J, Hou X, Wegener AM, Geisler C. CD3 gamma contains a phosphoserine-dependent di-leucine motif involved in down-regulation of the T cell receptor. *EMBO J*, 1994 May 1;13(9):2156-66.

26) Doyle DA, Morais Cabral J, Pfuetzner RA, Kuo A, Gulbis JM, Cohen SL, Chait BT, MacKinnon R. The structure of the potassium channel: molecular basis of K+ conduction and selectivity. *Science*, 1998;280(5360):69-77.

27) Dumay QC, Debut AJ, Mansour NM, Saier MH Jr. The copper transporter (Ctr) family of Cu+ uptake systems. *J Mol Microbiol Biotechnol*, 2006;11(1-2):10-9.

28) Eisses JF, Kaplan JH. Molecular characterization of hCTR1, the human copper uptake protein. *J Biol Chem*, 2002;277(32):29162-71.

29) Eisses JF, Chi Y, Kaplan JH. Stable plasma membrane levels of hCTR1 mediate cellular copper uptake. *J Biol Chem*, 2005a;280(10):9635-9.

30) Eisses JF, Kaplan JH. The mechanism of copper uptake mediated by human CTR1: a mutational analysis. *J Biol Chem*, 2005b;280(44):37159-68.

31) Eskelinen EL, Tanaka Y, Saftig P. At the acidic edge: emerging functions for lysosomal membrane proteins. *Trends Cell Biol*, 2003;13(3):137-45.

32) Furukawa Y, Torres AS, O'Halloran TV. Oxygen-induced maturation of SOD1: a key role for disulfide formation by the copper chaperone CCS. *EMBO J*, 2004;23(14):2872-81.

33) Gaetke LM, Chow CK. Copper toxicity, oxidative stress, and antioxidant nutrients. *Toxicology*, 2003;189(1-2):147-63.

34) Guo Y, Smith K, Lee J, Thiele DJ, Petris MJ. Identification of methionine-rich clusters that regulate copper-stimulated endocytosis of the human Ctr1 copper transporter. *J Biol Chem*, 2004;279(17):17428-33.

35) Haase H, Maret W. Partial oxidation and oxidative polymerization of metallothionein. *Electrophoresis*, 2008;29(20):4169-76.

36) Hamza I, Schaefer M, Klomp LW, Gitlin JD. Interaction of the copper chaperone HAH1 with the Wilson disease protein is essential for copper homeostasis. *Proc Natl Acad Sci U S A*, 1999;96(23):13363-8.

37) Hamza I, Prohaska J, Gitlin JD. Essential role for Atox1 in the copper-mediated intracellular trafficking of the Menkes ATPase. *Proc Natl Acad Sci U S A*, 2003;100(3):1215-20.

38) Haremaki T, Fraser ST, Kuo YM, Baron MH, Weinstein DC. Vertebrate Ctr1 coordinates morphogenesis and progenitor cell fate and regulates embryonic stem cell differentiation. *Proc Natl Acad Sci U S A*, 2007;104(29):12029-34

39) Horng YC, Cobine PA, Maxfield AB, Carr HS, Winge DR. Specific copper transfer from the Cox17 metallochaperone to both Sco1 and Cox11 in the assembly of yeast cytochrome C oxidase. *J Biol Chem*, 2004;279(34):35334-40.

40) Itoh S, Kim HW, Nakagawa O, Ozumi K, Lessner SM, Aoki H, Akram K, McKinney RD, Ushio-Fukai M, Fukai T. Novel role of antioxidant-1 (Atox1) as a copper-dependent transcription factor involved in cell proliferation. *J Biol Chem*, 2008;283(14):9157-67.

41) Itoh S, Ozumi K, Kim HW, Nakagawa O, McKinney RD, Folz RJ, Zelko IN, Ushio-Fukai M, Fukai T. Novel mechanism for regulation of extracellular SOD transcription and activity by copper: role of antioxidant-1. *Free Radic Biol Med*, 2009;46(1):95-104.

42) Jensen LT, Culotta VC. Activation of CuZn superoxide dismutases from Caenorhabditis elegans does not require the copper chaperone CCS. *J Biol Chem*, 2005;280(50):41373-9.

43) Kampfenkel K, Kushnir S, Babiychuk E, Inzé D, Van Montagu M. Molecular characterization of a putative Arabidopsis thaliana copper transporter and its yeast homologue. *J Biol Chem*, 1995;270(47):28479-86.

44) Kelleher SL, Lönnerdal B. Mammary gland copper transport is stimulated by prolactin through alterations in Ctr1 and Atp7A localization. *Am J Physiol Regul Integr Comp Physiol*. 2006;291(4):R1181-91.

45) Kim BE, Nevitt T, Thiele DJ. Mechanisms for copper acquisition, distribution and regulation. *Nat Chem Biol*, 2008;4(3):176-8.

46) Kim Guisbert KS, Li H, Guthrie C. Alternative 3' pre-mRNA processing in *Saccharomyces cerevisiae* is modulated by Nab4/Hrp1 in vivo. *PLoS Biol*, 2007;5(1):e6.

47) Kim H, Son HY, Bailey SM, Lee J. Deletion of hepatic Ctr1 reveals its function in copper acquisition and compensatory mechanisms for copper homeostasis. *Am J Physiol Gastrointest Liver Physiol*, 2009;296(2):G356-64.

48) Klomp AE, Tops BB, Van Denberg IE, Berger R, Klomp LW. Biochemical characterization and subcellular localization of human copper transporter 1 (hCTR1). *Biochem J*, 2002;364(Pt 2):497-505

49) Klomp AE, Juijn JA, van der Gun LT, van den Berg IE, Berger R, Klomp LW. The N-terminus of the human copper transporter 1 (hCTR1) is localized extracellularly, and interacts with itself. *Biochem J*, 2003;370(Pt 3):881-9.

50) Kubista H, Edelbauer H, Boehm S. Evidence for structural and functional diversity among SDS-resistant SNARE complexes in neuroendocrine cells. *J Cell Sci*, 2004 29;117(Pt 6):955-66.

51) Kuo YM, Zhou B, Cosco D, Gitschier J. The copper transporter CTR1 provides an essential function in mammalian embryonic development. *Proc Natl Acad Sci U S A*, 2001;98(12):6836-41.

52) Kuo YM, Gybina AA, Pyatskowit JW, Gitschier J, Prohaska JR. Copper transport protein (Ctr1) levels in mice are tissue specific and dependent on copper status. *J Nutr*, 2006;136(1):21-6

53) La Fontaine S, Mercer JF. Trafficking of the copper-ATPases, ATP7A and ATP7B: role in copper homeostasis. *Arch Biochem Biophys*, 2007;463(2):149-67.

54) Labbé S, Zhu Z, Thiele DJ. Copper-specific transcriptional repression of yeast genes encoding critical components in the copper transport pathway. *J Biol Chem*, 1997;272(25):15951-8.

55) Lee J, Prohaska JR, Dagenais SL, Glover TW, Thiele DJ. Isolation of a murine copper transporter gene, tissue specific expression and functional complementation of a yeast copper transport mutant. *Gene*, 2000;254(1-2):87-96.

56) Lee J, Prohaska JR, Thiele DJ. Essential role for mammalian copper transporter Ctr1 in copper homeostasis and embryonic development. *Proc Natl Acad Sci U S A*, 2001;98(12):6842-7.

57) Lee J, Peña MM, Nose Y, Thiele DJ. Biochemical characterization of the human copper transporter Ctr1. *J Biol Chem*, 2002a;277(6):4380-7.

58) Lee J, Petris MJ, Thiele DJ. Lee J, Petris MJ, Thiele DJ. Characterization of mouse embryonic cells deficient in the ctr1 high affinity copper transporter. Identification of a Ctr1-independent copper transport system. *J Biol Chem*, 2002b;277(43):40253-9.

59) Lee S, Howell SB, Opella SJ. NMR and mutagenesis of human copper transporter 1 (hCtr1) show that Cys-189 is required for correct folding and dimerization. *Biochim Biophys Acta*, 2007;1768(12):3127-34.

60) Liu J, Sitaram A, Burd CG. Regulation of copper-dependent endocytosis and vacuolar degradation of the yeast copper transporter, Ctr1p, by the Rsp5 ubiquitin ligase. *Traffic*, 2007;8(10):1375-84.

61) Lombardi D, Soldati T, Riederer MA, Goda Y, Zerial M, Pfeffer SR. Rab9 functions in transport between late endosomes and the trans Golgi network. *EMBO J*, 1993;12(2):677-82.

62) Lutsenko S, Gupta A, Burkhead JL, Zuzel V. Cellular multitasking: the dual role of human Cu-ATPases in cofactor delivery and intracellular copper balance. *Arch Biochem Biophys*, 2008;476(1):22-32.

63) Mackenzie NC, Brito M, Reyes AE, Allende ML. Cloning, expression pattern and essentiality of the high-affinity copper transporter 1 (ctr1) gene in zebrafish. *Gene*, 2004;328:113-20.

64) Madsen E, Gitlin JD. Copper and iron disorders of the brain. *Annu Rev Neurosci*, 2007;30:317-37.

65) Marks MS, Woodruff L, Ohno H, Bonifacino JS. Protein targeting by tyrosine- and di-leucine-based signals: evidence for distinct saturable components. *J Cell Biol*, 1996;135(2):341-54.

66) Maryon EB, Molloy SA, Kaplan JH. O-linked glycosylation at threonine 27 protects the copper transporter hCTR1 from proteolytic cleavage in mammalian cells. *J Biol Chem*, 2007;282(28):20376-87.

67) Minghetti M, Leaver MJ, Carpenè E, George SG. Copper transporter 1, metallothionein and glutathione reductase genes are differentially expressed in tissues of sea bream (Sparus aurata) after exposure to dietary or waterborne copper. *Comp Biochem Physiol C Toxicol Pharmacol*, 2008;147(4):450-9.

68) Miyashita T. Confocal microscopy for intracellular co-localization of proteins. *Methods Mol Biol*, 2004;261:399-410.

69) Møller LB, Petersen C, Lund C, Horn N. Characterization of the hCTR1 gene: genomic organization, functional expression, and identification of a highly homologous processed gene. *Gene*, 2000;257(1):13-22.

70) Nose Y, Kim BE, Thiele DJ. Ctr1 drives intestinal copper absorption and is essential for growth, iron metabolism, and neonatal cardiac function. *Cell Metab*, 2006;4(3):235-44.

71) Ogra Y, Aoyama M, Suzuki KT. Protective role of metallothionein against copper depletion. *Arch Biochem Biophys*, 2006;451(2):112-8.

72) O'Halloran TV, Culotta VC. Metallochaperones, an intracellular shuttle service for metal ions. *J Biol Chem*, 2000;275(33):25057-60.

73) Ohgami RS, Campagna DR, McDonald A, Fleming MD. The Steap proteins are metalloreductases. *Blood*, 2006;108(4):1388-94.

74) Ooi CE, Rabinovich E, Dancis A, Bonifacino JS, Klausner RD. Copper-dependent degradation of the Saccharomyces cerevisiae plasma membrane copper transporter Ctr1p in the apparent absence of endocytosis. *EMBO J*, 1996;15(14):3515-23.

75) Petris MJ, Smith K, Lee J, Thiele DJ. Copper-stimulated endocytosis and degradation of the human copper transporter, hCtr1. *J Biol Chem*, 2003;278(11):9639-46.

76) Pitcher C, Höning S, Fingerhut A, Bowers K, Marsh M. Cluster of differentiation antigen 4 (CD4) endocytosis and adaptor complex binding require activation of the CD4 endocytosis signal by serine phosphorylation. *Mol Biol Cell*, 1999;10(3):677-91.

77) Portnoy ME, Schmidt PJ, Rogers RS, Culotta VC. Metal transporters that contribute copper to metallochaperones in Saccharomyces cerevisiae. *Mol Genet Genomics*, 2001;265(5):873-82.

78) Potter SZ, Valentine JS. The perplexing role of copper-zinc superoxide dismutase in amyotrophic lateral sclerosis (Lou Gehrig's disease). *J Biol Inorg Chem*, 2003;8(4):373-80.

79) Prohaska JR. Role of copper transporters in copper homeostasis. *Am J Clin Nutr*, 2008;88(3):826S-9S.

80) Puig S, Lee J, Lau M, Thiele DJ. Biochemical and genetic analyses of yeast and human high affinity copper transporters suggest a conserved mechanism for copper uptake. *J Biol Chem*, 2002;277(29):26021-30.

81) Qin Z, Itoh S, Jeney V, Ushio-Fukai M, Fukai T. Essential role for the Menkes ATPase in activation of extracellular superoxide dismutase: implication for vascular oxidative stress. *FASEB J*, 2006;20(2):334-6.

82) Rae TD, Schmidt PJ, Pufahl RA, Culotta VC, O'Halloran TV. Undetectable intracellular free copper: the requirement of a copper chaperone for superoxide dismutase. *Science*, 1999;284(5415):805-8.

83) Rees EM, Lee J, Thiele DJ. Mobilization of intracellular copper stores by the ctr2 vacuolar copper transporter. *J Biol Chem*, 2004;279(52):54221-9.

84) Rees EM, Thiele DJ. Identification of a vacuole-associated metalloreductase and its role in Ctr2-mediated intracellular copper mobilization. *J Biol Chem*, 2007;282(30):21629-38

85) Riggio M, Lee J, Scudiero R, Parisi E, Thiele DJ, Filosa S. High affinity copper transport protein in the lizard Podarcis sicula: molecular cloning, functional characterization and expression in somatic tissues, follicular oocytes and eggs. *Biochim Biophys Acta*, 2002;1576(1-2):127-35.

86) Schröder B, Wrocklage C, Pan C, Jäger R, Kösters B, Schäfer H, Elsässer HP, Mann M, Hasilik A. Integral and associated lysosomal membrane proteins. *Traffic*, 2007;8(12):1676-86.

87) Son M, Puttaparthi K, Kawamata H, Rajendran B, Boyer PJ, Manfredi G, Elliott JL. Overexpression of CCS in G93A-SOD1 mice leads to accelerated neurological deficits with severe mitochondrial pathology. *Proc Natl Acad Sci U S A*, 2007;104(14):6072-7.

88) Song IS, Chen HH, Aiba I, Hossain A, Liang ZD, Klomp LW, Kuo MT. Transcription factor Sp1 plays an important role in the regulation of copper homeostasis in mammalian cells. *Mol Pharmacol*, 2008;74(3):705-13.

89) Sturtz LA, Diekert K, Jensen LT, Lill R, Culotta VC. A fraction of yeast Cu,Zn-superoxide dismutase and its metallochaperone, CCS, localize to the intermembrane space of mitochondria. A physiological role for SOD1 in guarding against mitochondrial oxidative damage. *J Biol Chem*, 2001 ;276(41):38084-9.

90) Suzuki KT. Disordered copper metabolism in LEC rats, an animal model of Wilson disease: roles of metallothionein. *Res Commun Mol Pathol Pharmacol,* 1995;89(2):221-40.

91) Takahashi Y, Kako K, Kashiwabara S, Takehara A, Inada Y, Arai H, Nakada K, Kodama H, Hayashi J, Baba T, Munekata E. Mammalian copper chaperone Cox17p has an essential role in activation of cytochrome C oxidase and embryonic development. *Mol Cell Biol*, 2002;22(21):7614-21.

92) Tennant J, Stansfield M, Yamaji S, Srai SK, Sharp P. Effects of copper on the expression of metal transporters in human intestinal Caco-2 cells. *FEBS Lett*, 2002;527(1-3):239-44.

93) van den Berghe PV, Folmer DE, Malingré HE, van Beurden E, Klomp AE, van de Sluis B, Merkx M, Berger R, Klomp LW Human copper transporter 2 is localized in late endosomes and lysosomes and facilitates cellular copper uptake. *Biochem J*, 2007;407(1):49-59.

94) Wernimont AK, Huffman DL, Lamb AL, O'Halloran TV, Rosenzweig AC. Structural basis for copper transfer by the metallochaperone for the Menkes/Wilson disease proteins. *Nat Struct Biol*, 2000;7(9):766-71.

95) Wong PC, Waggoner D, Subramaniam JR, Tessarollo L, Bartnikas TB, Culotta VC, Price DL, Rothstein J, Gitlin JD. Copper chaperone for superoxide dismutase is essential to activate mammalian Cu/Zn superoxide dismutase. *Proc Natl Acad Sci U S A*, 2000;97(6):2886-91.

96) Yamaguchi-Iwai Y, Serpe M, Haile D, Yang W, Kosman DJ, Klausner RD, Dancis A. Homeostatic regulation of copper uptake in yeast via direct binding of MAC1 protein to upstream regulatory sequences of FRE1 and CTR1. *J Biol Chem*, 1997;272(28):17711-8.

97) Wu X, Sinani D, Kim H, Lee J. Copper transport activity of yeast Ctr1 is down-regulated via its C terminus in response to excess copper. *J Biol Chem*, 2009;284(7):4112-22.

98) Xiao Z, Loughlin F, George GN, Howlett GJ, Wedd AG. C-terminal domain of the membrane copper transporter Ctr1 from *Saccharomyces cerevisiae* binds four Cu(I) ions as a cuprous-thiolate polynuclear cluster: sub-femtomolar Cu(I) affinity of three proteins involved in copper trafficking. *J Am Chem Soc*, 2004;126(10):3081-9.

99) Zeng L, Miller EW, Pralle A, Isacoff EY, Chang CJ. A selective turn-on fluorescent sensor for imaging copper in living cells. *J Am Chem Soc*., 2006;128(1):10-1.

100) Zhou B, Gitschier J. hCTR1: a human gene for copper uptake identified by complementation in yeast. *Proc Natl Acad Sci U S A*, 1997;94(14):7481-6.

101) Zhou H, Thiele DJ. Identification of a novel high affinity copper transport complex in the fission yeast *Schizosaccharomyces pombe*. *J Biol Chem*, 2001;276(23):20529-35

102) Zimnicka AM, Maryon EB, Kaplan JH. Human copper transporter hCTR1 mediates basolateral uptake of copper into enterocytes: implications for copper homeostasis. *J Biol Chem*, 2007;282(36):26471-80

APPENDIX

Development of a LC-mass based method for detection of PsP (Paralytic Shellfish Poisoning) biotoxins

INTRODUCTION

Algal biotoxins are small biomolecules produced by marine microalgae, responsible for food intoxications in human and animals and are divided in five groups, such as, PSP (Paralytic Shellfish Poisoning), DSP (Diarrhetic Shellfish Poisoning), ASP (Amnesic Shellfish Poisoning), NSP (Neurotoxic Shellfish Poisoning) e CFP (Ciguatera Fish Poisoning) (Hallegraeff, 2003).
The toxins belonging to the PsP group are mainly produced by marine dinoflagellates such as *Alexandrium catenella*, *A. cohorticula*, *A, fundyense*, *A. fraterculum*, *A. leei*, *A. minutum, A. tamarense, Gymnodinium catenatum* e *Pyrodinium bahamense* var. *compressum*.
Algal bloom can give rise to characteristic water colorations, known as "red tide", but an association between these events and production of biotoxins has not been established.
PsP group includes more than 21 highly hydrophobic toxins with a common tetrahydropurine backbone. Based on the functional group harbored in the side chain they can be divided in three groups: carbamoyl (R=$OCONH_2$) the most toxic, decarbamoyl (R=H) and N-sulfocarbamoyl (R= $OCONHSO_3^-$) the least toxic (Fig. 1). The most toxic PsP is saxitoxin, with a LD50 in the mouse dependent on the administration way: 10µg/Kg intraperitoneal, 263µg/Kg oral and <2µg/Kg respiratory.
Common symptoms following PsP intoxication include: nausea, vomiting, diarrhea, abdominal pain, and tingling or burning lips, gums, tongue, face, neck, arms, legs, and toes. Shortness of breath, dry mouth, a choking feeling, confused or slurred speech, and lack of coordination are also possible. Death can occur after 2-12h in case of ingestion of high concentrations of toxins as a result of respiratory block.
Italian and European legislations demand PsP analysis and quantitation on all seafood products (Rettifica del Regolamento (CE) n°853/2004 del Parlamento Europeo e del Consiglio; Regolamento (CE) n°2074/2005 della Commissione; Regolamento (CE) n°1664/2006 della Commissione; Gazzetta Ufficiale della Repubblica Italiana, 2002).
The official method for PsP identification is the mouse bioassay.
Recently a HPLC (High Pressure Liquid Chromatography) based method has been certified (Lawrence et al., 2005), but such method is time consuming and analysis of samples with complex toxin profiles can take up to three days of work.
My activity at the Centro Ricerche Marine-Cesenatico focused on the development of a LC-mass method to analyze and identify the biotoxins belonging to the PsP group as well as other hydrophilic algal bioxotins.

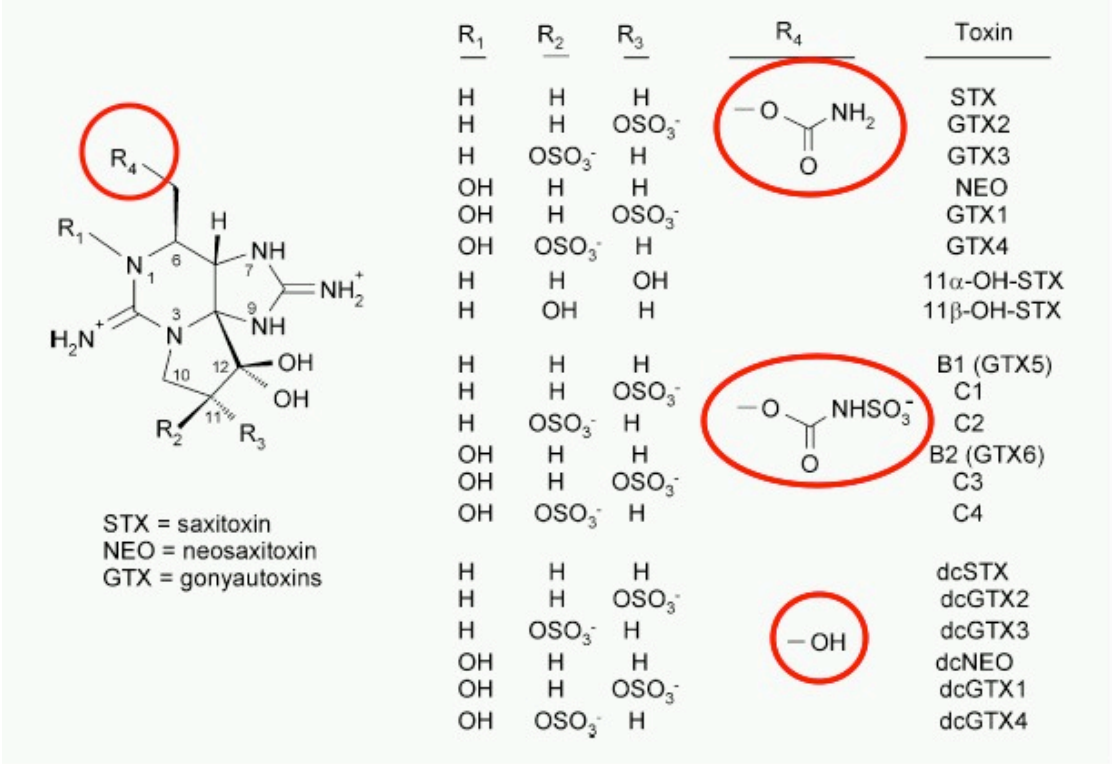

Figure 1. Chemical structure of PsP toxins.

MATERIALS AND METHODS

To set up and optimize the method it was used the following PsP certified standard (NRCC, National Research Council of Canada, Halifax): saxitoxin, (STX), neosaxitoxin (NEO), decarbamoylsaxitoxin (dcSTX), gonyautoxin 1-2-3-4(GTX1, GTX2, GTX3, GTX4), gonyautoxin 5 (B1), decarbamoylsaxitoxin 2 (dcGTX2) and decarbamoylsaxitoxin 3 (dcGTX3).
In addition we tested also certified standards of Domoic Acid (DA) e Tetradotoxin (TTX).
Mass spectral analyses were performed Varian 1200 L triple-quadruple, equipped with interface API/ESI. To increase the specificity of the signal we performed the analysis in selected reaction monitoring (SRM) and the transitions selected are reported in chromatograms.
To calibrate the instrument we infused in the mass spectrometer 1ppm of each standard and we acquired MS/MS breakdown plots in selected reaction monitoring mode (SRM) in positive and negative ion mode. For each standard we selected the transition with the highest intensity. Transitions selected are reported in chromatogram.
It was tested two different HILIC (Hydrophilic Interaction Chromatography) columns: a non-functionalized one (ATLANTIS™ HILIC Silica 5µm 2,1x150mm 100Å, Waters) and other harboring amide groups (TSK-GEL Amide-80 5µm 2,0x250mm, Tosoh Bioscience).
For each column we tested different mobile phases studying the effect of ACN percentage, pH, salt concentration and TFA addition on peak shape, resolution and sensitivity.
The optimized method involves the elution by gradient using the following mobile phases:
Mobile phase A**:** 64% ACN 36% H_20, 2mM ammonium formate 3,5mM formic acid
Mobile phase B**:** 64% ACN 36% H_20, 4mM ammonium formate 10mM formic acid, 0,01% TFA (trifluoroacetic acid).

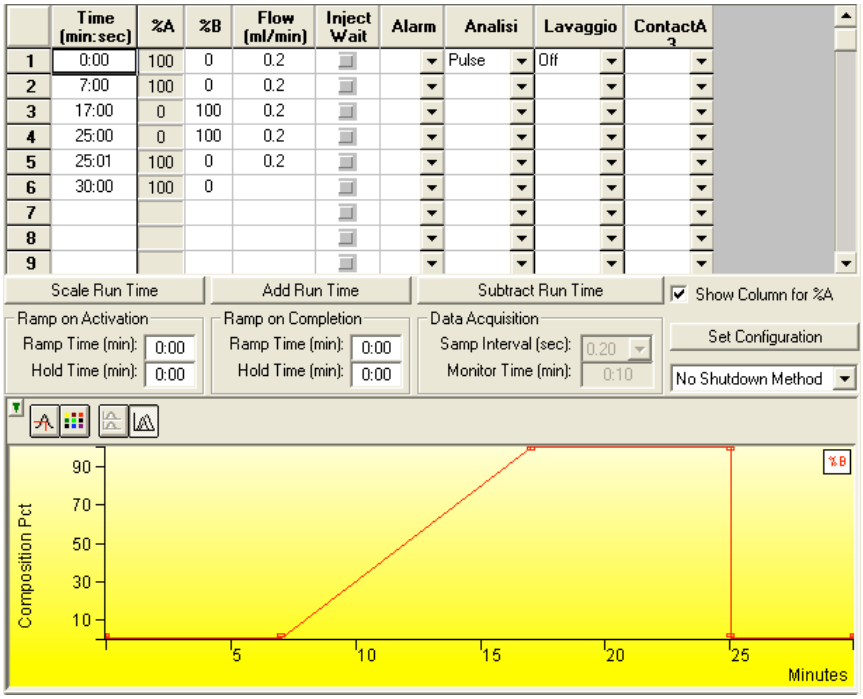

Figure 2. Scheme of the gradient employed in the method.

Two different SPE (solid phase extraction) cartridges were tested.
The first, a weak cation exchange column (BakerBond 500mg/3ml), was conditioned with 1ml of 0,01% ammonium formate, loaded with 1ml of sample, washed once with 1ml of water, further washed with 5mf ACN and eluted with 1ml of TFA 0,1%.
The second, a mixed mode cationic exchange (MCX Waters 60mg/3ml), was conditioned with MeOH 100%, equilibrated with 1ml 0,01% ammonium formate, loaded with 1ml of sample, washed once with 1ml of water, further washed with 1mf ACN and eluted with 1ml of TFA 0,1%.
Whole mussel soft tissues from negative samples were pooled and homogenized with a grinder.
5g of homogenate were extracted with 15ml of formic acid 0,1%, homogenizing 3min at 10000rpm with an Ultra Turrax and centrifugating at 3600rpm per 10min. The supernatant was contaminated with standards of STX and GTX1-4 at a final concentration of 1ppm each.

RESULTS AND DISCUSSIONS

HILIC chromatography was initially employed to separate and analyze by mass spectrometry peptides and nucleic acids, given its strong retention capacity for polar compounds and its high compatibility with ESI (electrospray ionization) technology (Alpert, 1990).
Analytes interact with a silica based stationary phase through hydrophilic interactions and probably ionic exchange interactions, the mobile phase containing a high percentage of organic solvents and low salt concentration favors ionization of the compounds in the ESI chamber.

As expected for both columns the retention times of the PsP toxins were proportional to the net charge of the compounds in the mobile phase. In the early stages of the research we employed an un-functionalized HILIC Column (Waters), already available in the laboratory.
Figure 3 shows a typical chromatogram of a PsP standard mixture using this column and applying the method proposed by Dell'Aversano et al., 2005. It is clear how this column cannot resolve toxins having the same net charge, like STX and NEO. Furthermore the single charged toxins, B1, GTX1-4 are not only not resolved, but are poorly retained by the column.
We then tested the TSK-GEL Amide-80, the same column employed in the published protocol, using the same chromatographic condition.
As expected for both columns the retention times of the PsP toxins were proportional to the net charge of the compounds in the mobile phase, but the TSK-GEL Amide-80 was significantly more efficient in retaining all the standards analyzed, indeed retention times of double charged toxins almost double increased of several minutes, and retention times of single charged toxins shifted from 4min to almost 10min (Fig. 4).

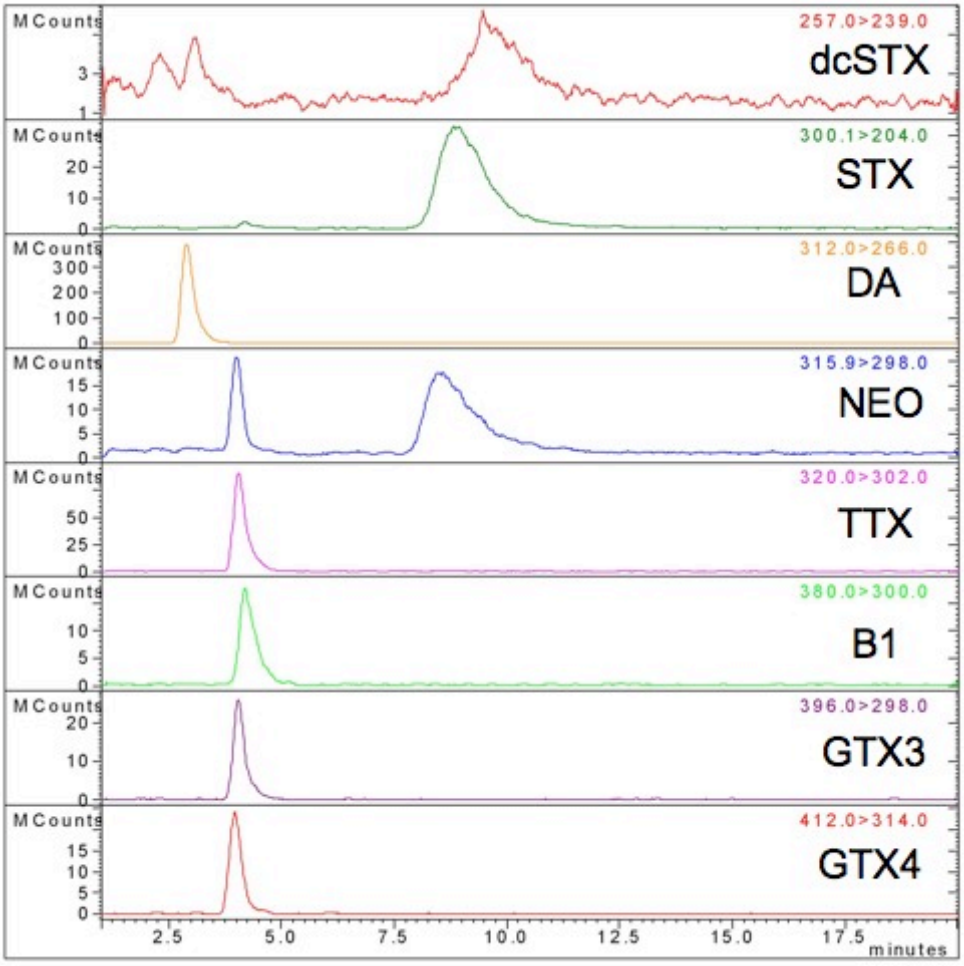

Figure 3. LC-mass analysis of a mixture of standards containing PsP toxins, Domoic Acid (DA) and Tetradotoin (TTX). Molecules were separated on an ATLANTIS™ HILIC Silica 5µm 2,1x150mm 100Å, column (Waters) using the method proposed by D'Aversano et al. (2005) and analyzed in SRM mode. For each standard the selected reaction is reported. Scales are not adjusted.

In HILIC percentage of organic phase is the critical factor affecting the separation, and even small variations can result in dramatic change. In general pH and salt concentration of the running buffer have a lower influence in retention times but they also have a critically impact in the ionization in the ESI chamber, consequently variations in these parameters can affect simultaneously retention times and signal intensities (Strege, 1998).
Despite the general improvement, it was observed a too broad peak shape of the double charged toxins that include the most toxic compounds. It was previously reported that TSK-GEL Amide-80 allows to selectively manipulating retention times by changes in the pH and salt concentration of the running buffer (Gou and Gaiki, 2005). Therefore it was decided to investigate the effect of these two factors.

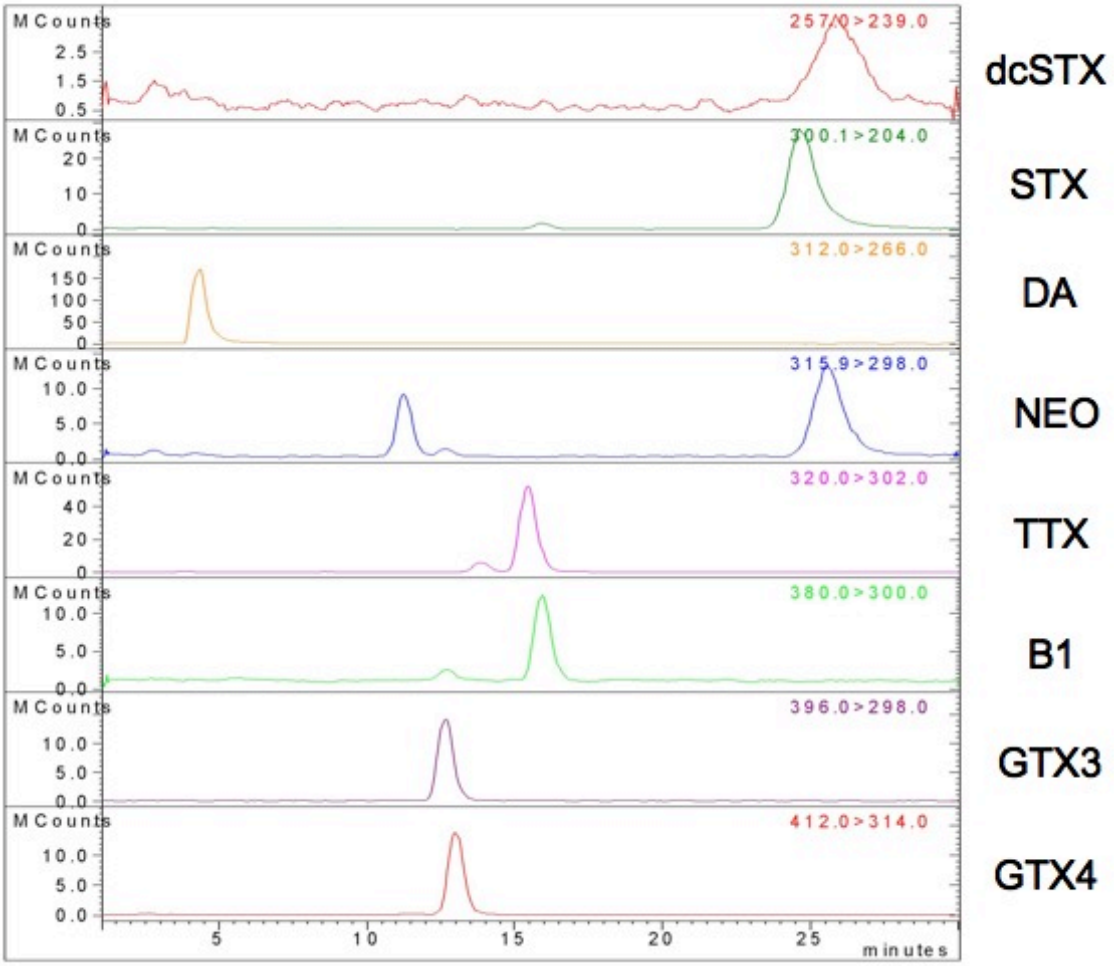

Figure 4. LC-mass analysis of a mixture of standards containing PsP toxins, Domoic Acid (DA) and Tetradotoin (TTX). Molecules were separated on a (TSK-GEL Amide-80 5µm 2,0x250mm, Tosoh Bioscience) using the method proposed by D'Aversano et al. (2005) and analyzed in SRM mode. For each standard the selected reaction is reported. Scales are not adjusted.

Lowering the pH decreased retention times of all the standards with a more marked effect on the double charged toxin, but in general it did not influence significantly the signal intensity (data not shown).

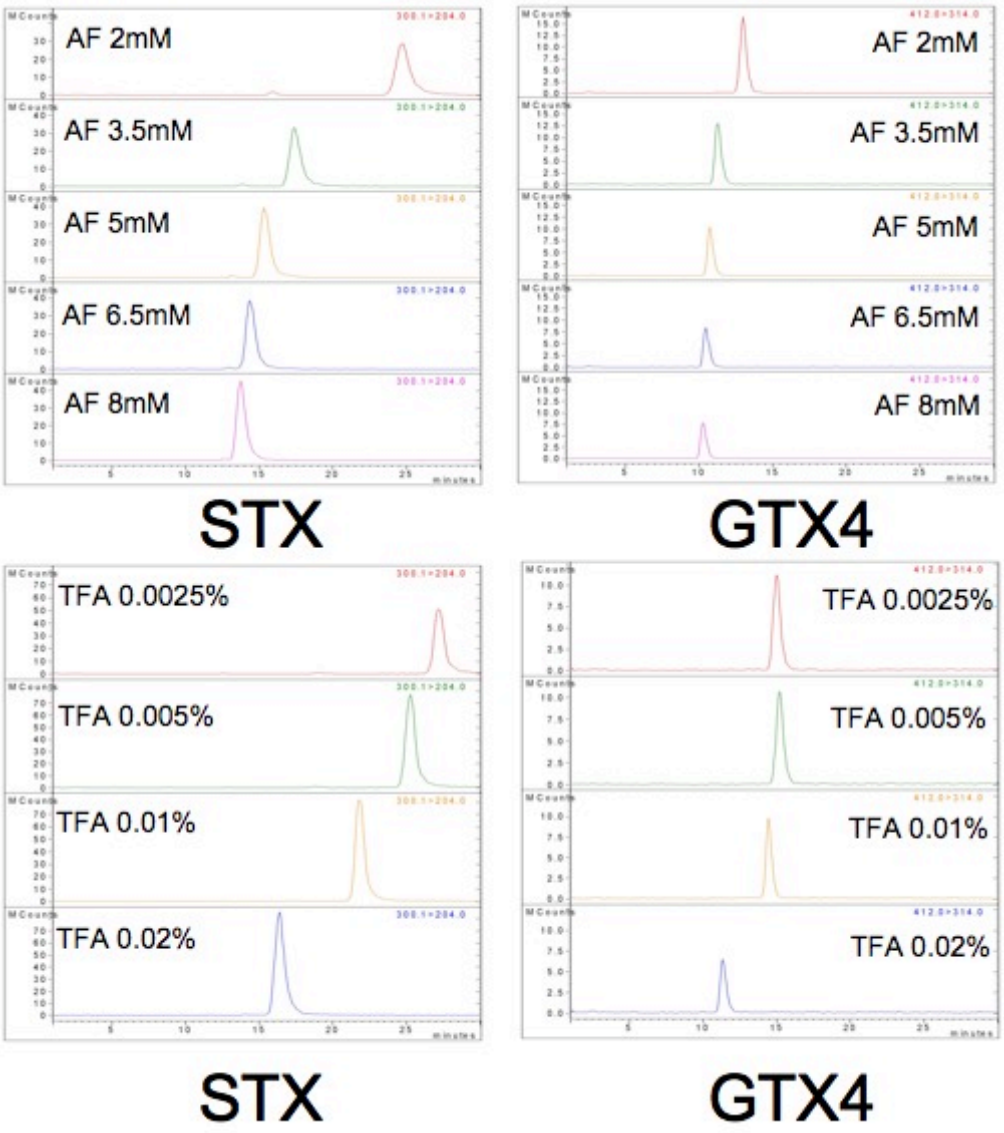

Figure 5. Effect of salt concentration (upper panels) and TFA addition (lower panels) in the mobile phase on the retention times and peak intensity of STX (left) and GTX4 (right). Scales are adjusted at the same level.

Small increases in the salt concentration had a significant effect on the retention times of the double charged compound STX: increasing the concentration of the ammonium formate from 2 to 8mM almost halved the retention time, improving peak shape and maximum peak intensity (Fig. 5 upper left panel).

The same variation in salt concentration had a similar but less pronounced effect on retention time of the single charged toxin GTX, but resulted in a strong reduction of the signal (Fig. 5 upper right panel).

The critical factor that dramatically improved the peak shape and signal intensity of the double charged PsP members (STX, NEO and dcSTX) was the employment in the mobile phase of low concentration of TFA (Fig. 5 lower panel).

It is likely that the interaction between the compounds and the column is mainly influenced by ionic bounds between the negatively charged silanol groups of the column and the positively charged guanidinic groups of the compounds.

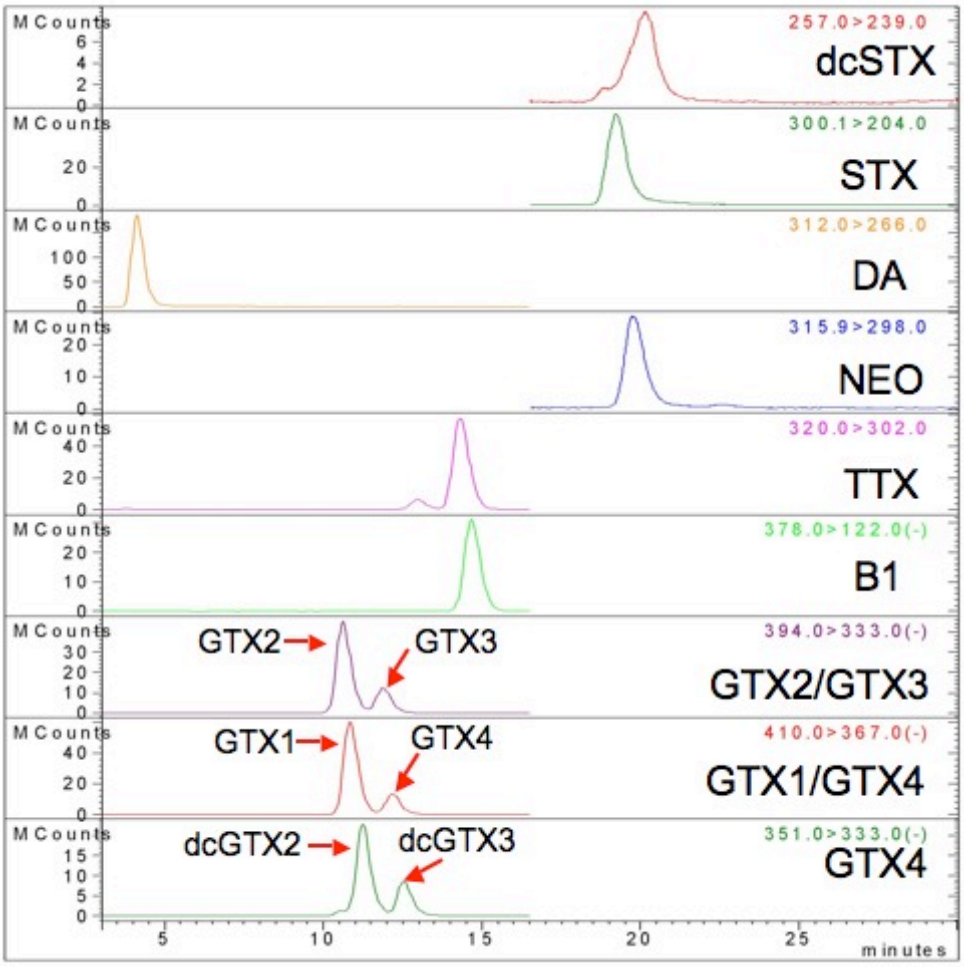

Figure 6. LC-mass analysis of a mixture of standards containing PsP toxins, Domoic Acid (DA) and Tetradotoin (TTX). Molecules were separated on a (TSK-GEL Amide-80 5µm 2,0x250mm, Tosoh Bioscience) using the method we developed and analyzed in SRM mode. For each standard the selected reaction is reported. Scales are not adjusted.

These ionic bounds probably cause the characteristic "tailing peak" observed for the double charged toxins and it is likely that TFA can inhibit such interactions resulting in a more symmetric peak.

Usually TFA, as other ion pairing agents, is not considered compatible with ESI ionization since it can induce a strong signal suppression, but recently it was shown that simultaneous use of TFA and other volatile acids such as ammonium formate, strongly reduces signal suppression (Shou and Naidong, 2005; Naldi *et al*., 2006).

Similarly to what observed with increasing salt concentrations, also addition of TFA caused a net decrease in signal intensity of single charged toxin (Fig. 5 lower panel).

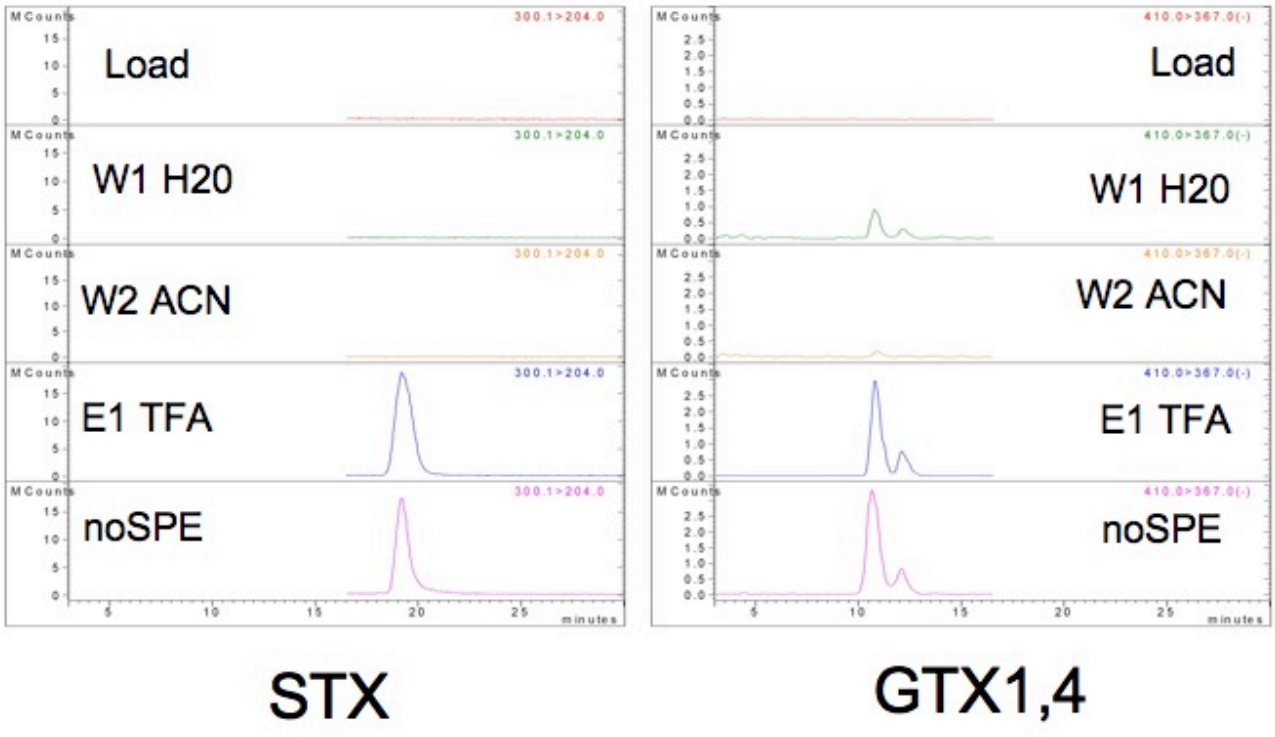

Figure 7. LC-mass analysis of a STX (left) and GTX1-4 (right) standard mixture was loaded on a weak ion exchange SPE cartridge (Bakerbon). Loadings, washes and eluates were separated on a (TSK-GEL Amide-80 5µm 2,0x250mm, Tosoh Bioscience) using the method developed and analyzed in SRM mode. The last row represents analysis of the amount of each standard identical to the one loaded on the SPE cartridges. For each standard the selected reaction is reported. Scales are not adjusted.

Given these results we figured that a gradient elution (Fig.1) would have been ideal in order to obtain a better elution and peak shape for double charged toxins without inducing signal suppression for the single charged toxin (Fig. 6).
Of the two SPE cartridges tested for sample preparations the cation exchange (Bakerbond) resulted in a good recover of STX and GTX (Fig. 7).
In the mixed mode cartridge elution of the double charged toxins was possible only using high salt concentrations or strong alkaline agents, that are not compatible with ESI analysis (data not shown).
Analysis of mussel extracts contaminated with PsP standards showed a matrix effect consistent in shifting of the retention times and especially signal suppression. Currently, we are investigating strategies to overcome such matrix effect.

REFERENCES

1) Alpert AJ. Hydrophilic-interaction chromatography for the separation of peptides, nucleic acids and other polar compounds. *J Chromatogr*, 1990; 499: 177-9

2) Dell'Aversano C, Hess P, Quilliam MA. Hydrophilic interaction liquid chromatography--mass spectrometry for the analysis of paralytic shellfish poisoning (PSP) toxins. *J Chromatogr A*., 2005; 1081(2): 190-201

3) Guo Y, Gaiki S. Retention behavior of small polar compounds on polar stationary phases in hydrophilic interaction chromatography. *J Chromatogr A*, 2005; 1074(1-2): 71-80

4) Hallegraeff GM (2003). Harmful algal blooms: a global overview. In: Hallegraeff G.M., Anderson D.M. and Cembella A.D. (eds), Manual on Harmful Marine Microalgae. Paris, UNESCO Publishing, pp. 25-49

5) Lawrence JF, Niedzwiadek B, Menard. Quantitative determination of paralytic shellfish poisoning toxins in shellfish using prechromatographic oxidation and liquid chromatography with fluorescence detection: collaborative study. *J AOAC Int*, 2005; 88(6): 1714-1732

6) Naldi M., Andrisano V., Fiori J., Calonghi N., Pagnotta E., Parolin C., Pieraccini G., Masotti L. (2006). Histone proteins determined in a human colon cancer by high-performance liquid chromatography and mass spectrometry. *J Chromatogr A*, 2006; 1129(1): 73-81.

7) Shou WZ, Naidong W. Simple means to alleviate sensitivity loss by trifluoroacetic acid (TFA) mobile phases in the hydrophilic interaction chromatography-electrospray tandem mass spectrometric (HILIC-ESI/MS/MS) bioanalysis of basic compounds. *J Chromatogr A*, 2005;825(2): 186-92.

8) Strege MA (1998). Hydrophilic interaction chromatography-electrospray mass spectrometry analysis of polar compounds for natural product drug discovery. Anal chem, 1998;70: 2439-2445.